Photosynth Res (2016) 130:193–213
DOI 10.1007/s11120-016-0243-0

ORIGINAL ARTICLE

The slow phase of chlorophyll *a* fluorescence induction in silico: Origin of the S–M fluorescence rise

Alexandrina Stirbet[1] · **Govindjee**[2]

Received: 3 December 2015 / Accepted: 4 March 2016 / Published online: 19 March 2016
© Springer Science+Business Media Dordrecht 2016

Abstract In higher plants, algae, and cyanobacteria, chlorophyll (Chl) *a* fluorescence induction (ChlFI) has a fast (under a second) increasing OJIP phase and a slow (few minutes) PS(M)T phase, where O is for origin, the minimum fluorescence, J and I for intermediate levels, P for peak, S for a semi-steady state, M for a maximum (which is sometimes missing), and T for the terminal steady-state level. We have used a photosynthesis model of Ebenhöh et al. (Philos Trans R Soc B, 2014, doi:10.1098/rstb.2013.0223) in an attempt to simulate the slow PS(M)T phase and to determine the origin of the S–M rise in *Chlamydomonas* (*C.*) *reinhardtii* cells. Our experiments in silico show that a slow fluorescence S–M rise (as that observed, e.g., by Kodru et al. (Photosynth Res 125:219–231, 2015) can be simulated only if the photosynthetic samples are initially in a so-called "state 2," when the absorption cross section (CS) of Photosystem II (PSII) is lower than that of PSI, and Chl *a* fluorescence is low (see, e.g., a review by Papageorgiou and Govindjee (J Photochem Photobiol B 104:258–270, 2011). In this case, simulations show that illumination induces a state 2 (s2) to state 1 (s1) transition (qT_{21}), and a slow S–M rise in the simulated ChlFI curve, since the fluorescence yield is known to be higher in s1, when CS of PSII is larger than that of PSI. Additionally, we have analyzed how light intensity and several photosynthetic processes influence the degree of this qT_{21}, and thus the relative amplitude of the simulated S–M phase. A refinement of the photosynthesis model is, however, necessary in order to obtain a better fit of the simulation data with the measured ChlFI curves.

Keywords Anoxia · *Chlamydomonas reinhardtii* · Mathematical simulation · Nonphotochemical quenching · Photosynthesis model · Slow Chl *a* fluorescence induction · State transitions

Abbreviations

A	Antheraxanthin
CET1	Cyclic electron transport around PSI
Chl	Chlorophyll
Cyt	Cytochrome
CS	Absorption cross section
F_0	Minimum Chl *a* fluorescence
Fd	Ferredoxin
F_M	Maximum Chl *a* fluorescence
FNR	Ferredoxin-$NADP^+$ oxidoreductase

This paper is dedicated to George C. Papageorgiou, who, together with one of us (Govindjee), had made, during 1967–1968, pioneering observations on the slow S (steady state) to M (maximum) fluorescence rise phase in algae and cyanobacteria. Exceptional achievements of George in photosynthesis research were recently celebrated during an international conference on "Photosynthesis research for sustainability-2015" in Crete, Greece (see an account in Allakhverdiev et al. (2015), and http://photosynthesis2015.cellreg.org/Programme.php).

Guest Editor: Kostas Stamatakis.

Electronic supplementary material The online version of this article (doi:10.1007/s11120-016-0243-0) contains supplementary material, which is available to authorized users.

✉ Govindjee
gov@illinois.edu

Alexandrina Stirbet
sstirbet@gmail.com

[1] 204 Anne Burras Ln, Newport News, VA 23606, USA

[2] Department of Biochemistry, Department of Plant Biology, and Center of Biophysics & Quantitative Biology, University of Illinois at Urbana-Champaign, Urbana, IL 61801-3707, USA

FQR	Ferredoxin:plastoquinone oxidoreductase
k_D	Rate constant of heat dissipation
k_F	Rate constant of fluorescence
LHC	Light-harvesting complex
NDA2	A monomeric type-II NA(D)H dehydrogenase
NADP	Nicotinamide adenine dinucleotide phosphate
NPQ	Nonphotochemical quenching of excited state of Chl
ODEs	Ordinary differential equations
P680	Reaction center of PSII
P700	Reaction center of PSI
PBS	Phycobilisome
PC	Plastocyanin
PFD	Photon flux density
PQ	Plastoquinone
PS	Photosystem
PTOX	Plastid terminal oxidase
Q_o	Oxidizing site of PQH_2 on Cyt *b6f*
Q_A	Primary PSII plastoquinone (electron) acceptor
Q_B	Secondary PSII plastoquinone (electron) acceptor
qE	High-energy NPQ
qT	State transition related change
Stt7 (and STN7)	LHCII kinases required for phosphorylation of mobile LHCII in *Chlamydomonas reinhardtii* (and in *Arabidopsis thaliana*)
Pph1 and TAP38	LHCII phosphatases required for dephosphorylation of mobile LHCII
V	Violaxanthin
Z	Zeaxanthin

Introduction

When photosynthetic samples are illuminated with constant continuous light, chlorophyll (Chl) *a* fluorescence intensity undergoes characteristic changes, a phenomenon called the Kautsky effect (Kautsky and Hirsh 1931) or Chl *a* fluorescence induction; see also http://www.fluoromatics.com/kautsky_effect.php). In dark-adapted higher plants and algae, this fluorescence transient has a fast (hundreds of milliseconds) increasing phase, until a peak P is reached, followed by a slow (few minutes) decreasing phase, which often shows a transient maximum M; in contrast, M is much higher in cyanobacteria than the P level (cf. Fig. 1a, with Fig. 1b, plotted both on log and linear time scales). Several inflection points (e.g., J & I) are observed in Chl *a* fluorescence induction curves, shown in Fig. 1 (Govindjee 1995). The fast phase is usually called OJIP (Strasser and Govindjee 1991), where O is for origin, the minimum fluorescence F_0, J and I are intermediate levels, and P is the peak (which under saturating light conditions is the maximum fluorescence, F_M), while the slow phase is called PS(M)T (Papageorgiou and Govindjee 1968a, b), where S stands for a semi-steady state, M for a maximum (which sometimes is missing, as in Fig. 1a, curve *HL*), and T for a terminal steady-state level. Moreover, under certain conditions, e.g., sudden transition from low to high light, or change in $[CO_2]$, Chl *a* fluorescence induction curve shows several slow ($\sim$60 s) damped oscillations, together with antiparallel oscillations in oxygen evolution and CO_2 uptake or in other related metabolite pools (see e.g., Van der Veen 1949; Walker 1992; Lazár 1999; Stirbet et al. 2014).

The measurement of Chl *a* fluorescence transient is a noninvasive and highly sensitive technique, which is used extensively in the study of photosynthesis (see, e.g., chapters in Govindjee et al. 1986; Papageorgiou and Govindjee 2004), particularly for Photosystem II (PSII) activity, since PSI fluorescence is practically constant (Mar et al. 1972; Briantais et al. 1972; Kitajima and Butler 1975; for a different opinion, see Lazár 2013) and significantly lower than that of PSII at room temperature. Cyanobacteria differ from higher plants and algae, as in their case Chl *a* fluorescence is mainly sensitized by phycobilins, the direct Chl *a* fluorescence contribution to the total fluorescence signal being small (see discussion in Papageorgiou et al. 2007).

According to Duysens and Sweers (1963), Chl *a* fluorescence rise from F_0 (the minimum) to F_M (the maximum), during the fast OJIP phase, is a monitor of the accumulation in time of net reduced primary plastoquinone acceptor (Q_A^-) in PSII centers (see a discussion in Stirbet and Govindjee 2012).

The slow PS(M)T phase, a name coined by Papageorgiou and Govindjee (1968a, b), was first systematically studied in the *Photosynthesis Lab* at the University of Illinois, Urbana-Champaign (e.g., Govindjee and Papageorgiou 1971; Mohanty and Govindjee 1973; Mohanty et al. 1973). The shape of this phase depends greatly on the nature and history of the photosynthetic organism. In higher plants, the slow S–M rise is not always present, but a small fluorescence increase, centered at $\sim$10 s, can be observed under low light (see Fig. 1a; Strasser et al. 1995). On the other hand, the SMT phase is predominant in cyanobacteria, with the maximum M at $\sim$ 200 s, and with an M level much higher than the peak P (Fig. 1b; Tsimilli-Michael et al. 2009). In *Chlamydomonas* (*C.*) *reinhardtii* cells grown under low light and dark adapted for 5 min, the S–M rise is not very prominent, the M level reaching after $\sim$ 100 s (see, e.g., Zhou et al. 2010, 2015). However, when *C. reinhardtii* cells are dark adapted for 45 min

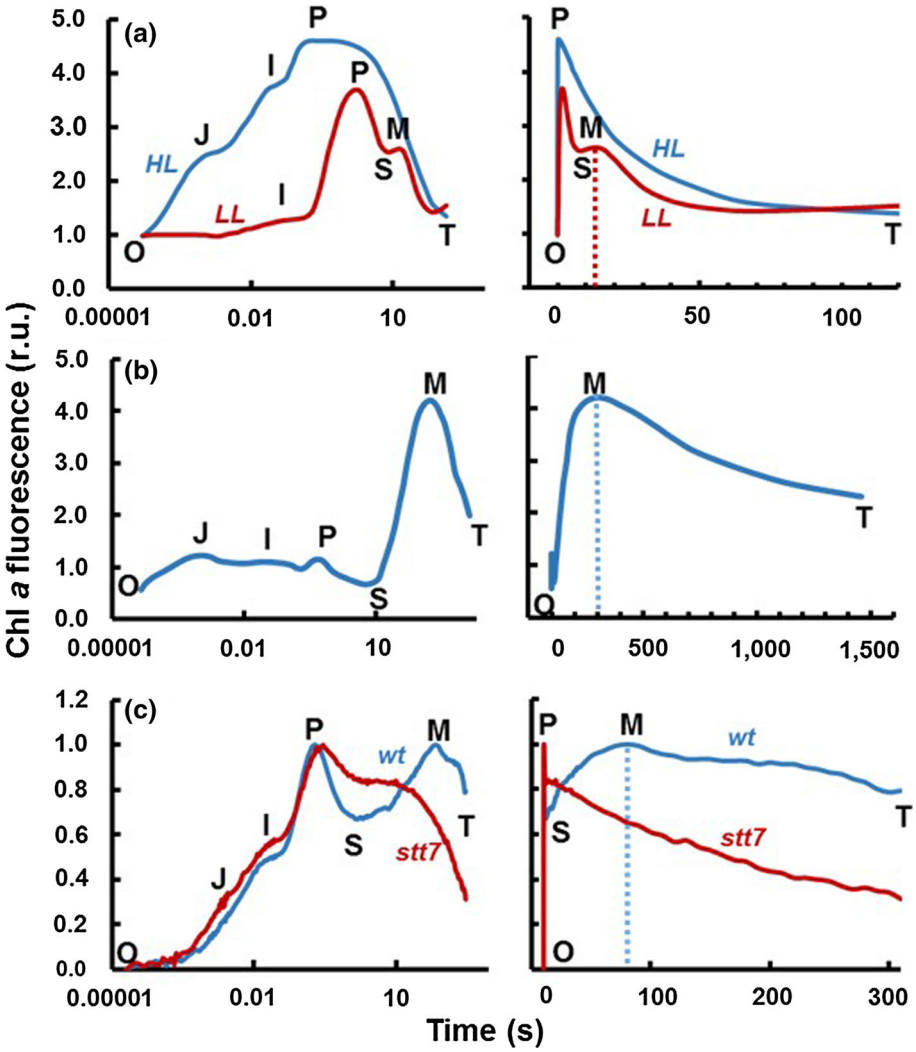

Fig. 1 Chlorophyll (Chl) *a* fluorescence transients of different photosynthetic organisms measured with a PEA (Photosynthetic Efficiency Analyser, Hansatech, UK) instrument under continuous red light; *left curves* are on log (time) scales, while the *right curves* are on linear (time) scales. The transients shown in **a** were measured in leaves of *Pisum sativum* under 3000 (HL) and 300 µmol photons m^{-2} s^{-1} (LL) (redrawn from Strasser et al. 1995); **b** *Synechococcus* sp. PCC 7942 cells (redrawn from Tsimilli-Michael et al. 2009); and **c** wild type (wt) and stt mutant of *C. reinhardtii* cells dark adapted for 45 min without agitation (redrawn from Kodru et al. 2015). The O, J, I, P, S, M, and T steps (O, for origin, is the first measured minimum fluorescence level; P is the peak; S stands for semi-steady-state level; M is for maximum, and T is for terminal steady state) are marked in the figure; r.u. stands for relative units

without agitation, the amplitude of the S–M rise increases, with the maximum M reaching the P level (curve *wt* in Fig. 1c; Kodru et al. 2013, 2015), while, under the same conditions, the S–M rise is completely missing in the stt7 mutant, which is locked in state 1 (Fig. 1c, curve *stt*). Further, Kodru et al. (2015) also found that the M level is lowered after chemical treatments that induce nonphotochemical reduction of the plastoquinone (PQ) pool (an intersystem electron carrier).

During the slow PS(M)T phase, Chl *a* fluorescence is modulated not only by photochemical quenching (i.e., quenching by Q_A) but also, directly or indirectly, by other photosynthetic processes, such as: high-energy nonphotochemical quenching (NPQ) of singlet excited Chl *a* (^{1}Chl *a**) in PSII antenna (i.e., qE, a fast forming NPQ induced by low pH in lumen, rapidly reversible in darkness; see a review by Papageorgiou and Govindjee 2014), photoinhibition (i.e., qI, a slow-forming NPQ due to PSII photodamage, mostly irreversible in darkness; Tyystjärvi et al. 2005; Murata et al. 2012; Tyystjärvi 2013), state transitions (i.e., qT, a regulatory adjustment of the excitation energy distribution between PSI and PSII, slowly reversible in darkness; Rochaix 2014), carbon assimilation during Calvin–Benson (CB) cycle, photorespiration, and chlororespiration (see reviews by Papageorgiou et al. 2007 and Stirbet et al. 2014).

Both qE and qT are short-term mechanisms that regulate the light-harvesting capacity of the two photosystems, in

order to efficiently balance the input and utilization of light energy and to reduce photooxidative events that can damage the reaction centers (see chapters in Demmig-Adams et al. 2014). The relative contribution of these regulatory processes to the fluorescence modulation is strongly dependent on the preillumination history, quality (wavelength) of the illumination, as well as the intensity and duration of light exposure. In cyanobacteria, orange carotenoid protein (OCP)-related photoprotection and state transitions (involving the movement of phycobilisomes (PBS) or photosystems) optimize the energy distribution between the two photosystems (see a review by Kirilovsky 2015; see also, e.g., Leverenz et al. 2015; Steinbach et al. 2015; Zhao et al. 2015). Below we will briefly discuss qE and qT only in higher plants and algae.

During qE, which is triggered by low lumenal pH (Briantais et al. 1979), the de-excitation of singlet excited ^{1}Chl* by internal conversion (heat loss) in PSII antenna increases, and thus Chl *a* fluorescence is quenched. The mechanism of qE is species dependent (see, e.g., Niyogi and Truong 2013). In higher plants and some algae, it involves quenching that depends on PsbS (Li et al. 2000; Goral et al. 2012; for a theoretical approach, see Lambrev et al. 2012) or on Light-Harvesting Complex Stress-Related (LHCSR) proteins (Peers et al. 2009; Bonente et al. 2011; Tokutsu and Minagawa 2013). Further, in brown algae and diatoms, this depends on fucoxanthin and Chl a/c proteins (see, e.g., Alami et al. 2012), and in several cases, quenching is also by zeaxanthin (qZ), lutein (qL), or diadinoxanthin (qD) [see reviews by Jahns and Holzwarth (2012); Papageorgiou and Govindjee (2014)].

As mentioned earlier, state transitions fine-tune the distribution of excitation energy between PSI and PSII, providing balanced photosynthesis. It is generally assumed that micro- and macro-structural changes in the thylakoid membrane (Iwai et al. 2014) lead to equilibration of PSII and PSI activities through adjustment of their relative absorption cross sections (CS): CSII decreases and CSI increases during state 1-to-2 transition (qT_{12}), when Chl *a* fluorescence yield decreases, while the opposite happens during state 2-to-1 transition (qT_{21}), when Chl *a* fluorescence yield increases (Murata 1969a, b; Bonaventura and Myers 1969). State transitions are regulated by the redox state of the PQ pool, the controlling event taking place at the Qo site of cytochrome (Cyt) *b6f* (i.e., the binding site of plastoquinol (PQH_2); Zito et al. 1999); during illumination, qT_{12} is triggered by a reduced PQ pool, when PSII transfers electrons faster than PSI, whereas qT_{21} is triggered by an oxidized PQ pool (when PSI transfers electrons faster than PSII). However, we note that state transitions are also triggered by nonphotochemical oxidation or reduction of the PQ pool in darkness (see e.g., Bulté et al. 1990). In higher plants and algae, the controlling event of state transitions is generally assumed to be the redox activation/deactivation of a LHCII kinase, depending on the occupancy of the Qo site of Cyt *b6f* (see Fig. 2; Bennett et al. 1980; Allen et al. 1981; Allen 1992; Rochaix 2014); the LHCII kinase was identified as STN7 in Arabidopsis and as Stt7 in Chlamydomonas (Lemeille and Rochaix 2010; Rochaix 2013, 2014). Under excess PSII light, PQ pool is reduced; this activates a kinase, which triggers qT_{12} (state 1 to state 2 transition); mobile LHCIIs are phosphorylated, which dissociate from PSII and then associate with PSI (Andersson et al. 1982; Kouřil et al. 2005; Kargul et al. 2005). On the other hand, under excess PSI light, PQ pool is oxidized; this inactivates the kinase, but allows the redox-independent phosphatase (PPH1 or TAP38; Silverstein et al. 1993; Shapiguzov et al. 2010; Pribil et al. 2010) to dephosphorylate the phosphorylated mobile LHCIIs, which then dissociate from PSI and associate with PSII; this is qT_{21}, state 2 to state 1 transition. Alternatively, in higher plants, LHCII kinase may be also inhibited by the ferredoxin-thioredoxin system under high intensity white light (Rintamäki et al. 2000). At the end of state transitions, the PQ pool reaches a new redox poise and the imbalance between PSI and PSII activities is corrected. However, we note that an alternative view on qT (i.e., energy spillover; Murata 1969a, b; Mohanty et al. 1973; Butler and Kitajima 1975; Kitajima and Butler 1975) is being discussed again (see Grieco et al. 2015); in this view, the transfer of phosphorylated/dephosphorylated mobile LHCIIs between the two photosystems during state transitions is not necessary; instead, an equilibration of PSI and PSII activities is achieved, mostly in the grana margins, through a transfer of excitation energy between the two photosystems, which is facilitated by a network of free LHCII trimers.

Soon after the discovery of state transitions by Murata (1969a, 1969b) and Bonaventura and Myers (1969), the slow S–M fluorescence rise was suggested to be correlated with a state 2-to-1 transition, since both oxygen evolution and fluorescence increase in parallel (Govindjee and Papageorgiou 1971). Kaňa et al. (2012) have elegantly established that in cyanobacteria, which are usually in state 2 in darkness and have a high PSI/PSII ratio, the origin of their predominant slow S–M fluorescence rise (see Fig. 1b) is a state 2-to-1 transition, as the S–M rise is absent in the RpaC$^-$ mutant, locked in state 1, and in cells kept in hyperosmotic suspension, locked in state 2.

Allorent et al. (2013) measured Chl *a* fluorescence quenching dynamics in wild-type cells of the green alga *C. reinhardtii* previously acclimated for 4 h in high light, and earlier in state 2 after dark-adaptation. (For a review on Chl *a* fluorescence quenching dynamics, see Lazár 2015.) During illumination with actinic light, these samples showed, after an initial decrease due to qE, a slow (tens of

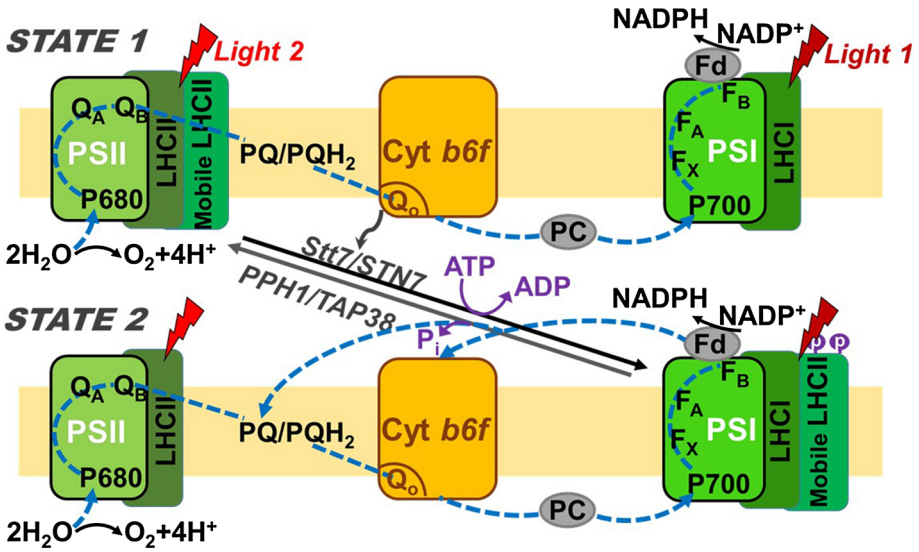

Fig. 2 The molecular basis of state transitions in higher plants and algae (see explanation in the main text). *PSII and PSI*: photosystem II and I; *P680 and P700*: reaction centers of PSII and PSI; Q_A *and* Q_B: primary and secondary PSII plastoquinone acceptors; *LHCII and LHCI*: light-harvesting complexes of PSII and PSI; *PQ and* PQH_2: oxidized and reduced plastoquinone; *Cyt*: cytochrome; *Qo*: PQH_2-oxidizing site of Cyt *b6f*; *PC*: plastocyanin; F_X, F_A, F_B: Iron sulfur proteins; *Fd*: ferredoxin; *NADP*: nicotinamide adenine dinucleotide phosphate; *Stt7* (in *Chlamydomonas reinhardtii*) and STN7 (*in Arabidopsis thaliana*): LHCII kinases for phosphorylation of mobile LHCII; *Pph1 and TAP38*: LHCII phosphatases for dephosphorylation of mobile LHCII. Figure modified from Allen (2003) and Rochaix (2014)

seconds) transitory increase in the fluorescence yield, which was correlated with a state 2-to-1 transition.

Ebenhöh et al. (2014) showed similar Chl *a* fluorescence quenching dynamics in wild-type *C. reinhardtii* cells grown in low light, which were kept for 10 min in anoxic conditions under dim light, and then exposed to actinic light in the presence of oxygen. Indeed, after the transition of these cells to state 2 (that is usually induced in darkness or dim light when the oxygen is very low or missing; Bulté et al. 1990), subsequent illumination under aerobic conditions led to an increase in the fluorescence yield, which was attributed to a state 2-to-1 transition. Further, Ebenhöh et al. (2014) compared their experimental results with theoretically simulated curves that were calculated using a basic photosynthesis model in which, for the first time, both high-energy NPQ (qE) and state transitions (qT) were included.

In our paper, the model of Ebenhöh et al. (2014), which had been conceived and used to simulate Chl *a* fluorescence quenching dynamics, was adapted to allow the simulation of Chl *a* fluorescence transients measured under continuous illumination (see details in "Appendix"). Our main goal here is to examine the origin of the S–M fluorescence rise that is observed in Chl *a* fluorescence induction curves (see e.g., Fig. 1c, and Fig. 1d) and to analyze the factors that influence this phase. Several attempts have been made in the past to simulate the slow PS(M)T phase using mathematical models of various complexities or by fitting the Chl *a* fluorescence transient using a set of mathematical expressions, but without considering state transitions, and only for higher plants (see e.g., Laisk et al. 2006; Zhu et al. 2013; Tanabe et al. (personal communication, 2015[1]); Belyaeva et al. (personal communication, 2015[2])). For a discussion of the use of models in understanding photosynthesis, see chapters in Laisk et al. (2009). Here, we have used the photosynthesis model of Ebenhöh et al. (2014) to simulate Chl *a* fluorescence transient curves in *C. reinhardtii* cells, under continuous light and under aerobic conditions, after different periods of dark-adaptation in the absence of oxygen. Our simulations show that, indeed, a state 2-to-1 transition can be induced only in samples that are initially in state 2, and that this state change is the origin of the slow S–M fluorescence rise, but under the condition that the initial absorption cross section of PSII is <0.5. We have also analyzed here different factors that influence the relative amplitude of the simulated S–M rise phase. However, the subsequent M–T fluorescence decrease observed in experimental Chl *a* fluorescence induction curves (see, e.g., Fig. 1c, and Fig. 1d) is missing in all simulated curves, even in the presence of qE. Although we are able to show

[1] Tanabe T, Tsunoda T, Hiyama T, Fukuda M (2015) Slow phase signal enhancement method using convolution for chlorophyll fluorescence. Presented at the International Conference of Photosynthesis Research for Sustainability, Crete, Greece.

[2] Belyaeva NE, Bulychev AA, Riznichenko GYu, Rubin AB (2015) Analysis of charge fluxes in thylakoid based on the photosystem II electron transfer modeling. Presented at the International Conference of Photosynthesis Research for Sustainability, Crete, Greece.

that the S–M fluorescence rise is due to a state 2 to state 1 transition, further research is needed to obtain a better fit by formulating and using a more detailed model.

The photosynthesis model of Ebenhöh et al. (2014)

Ebenhöh et al. (2014) had used their model to simulate Chl a fluorescence quenching dynamics measured with a pulse amplitude modulation (PAM) Fluorescence Monitoring System (Hansatech, UK); however, we have modified it to allow us to calculate Chl *a* fluorescence transients measured in continuous light (see details in "Appendix"). In their model, the authors took into account processes involved in short-term regulation of the photosynthetic electron transfer chain to changing light, as shown in a diagram in Fig. 3 (see also Table 1 in the "Appendix"). Besides the linear electron transport from water to nicotinamide adenine dinucleotide phosphate ($NADP^+$), there is also cyclic electron transport around PSI (CET1), as well as chlororespiration. Further, Ebenhöh and coworkers included the pH change in the lumen (with pH in stroma being assumed constant, for simplicity), ATP synthesis, state transitions (qT), and energy-dependent NPQ (qE). Finally, the consumption of both ATP and NADPH in the Calvin–Benson cycle and other metabolic processes was taken into account, but only implicitly; for simplicity, these were considered to be first-order reactions, but without any light activation period.

Since Ebenhöh and coworkers dealt mainly with processes taking place in seconds to minutes, their model did not include a detailed description of the photosynthetic complexes, which were treated as oxidoreductases; for example, PSII is described as a light-dependent water (H_2O)-plastoquinone (PQ) oxidoreductase (Fig. 4a), and PSI as a light-dependent plastocyanin (PC)-ferredoxin (Fd) oxidoreductase (Fig. 4b). Note that PQ reduction by Q_A^- in PSII (i.e., the two-electron gate mechanism; Bouges-Bocquet 1973; see a review on PSII by Govindjee et al. 2010) was approximated by two successive reduction(s) of a half of a PQ molecule. However, using this approach, the potential effects of PQ binding to the Q_B site and the release of PQH_2 from the Q_B site have been disregarded; these need to be considered in a future refined model.

Reflecting on the existing experimental evidence, qE in this model is induced by low lumenal pH that leads to the generation of zeaxanthin (*Z*) through de-epoxidation of violaxanthin (*V*) via antheraxanthin (*A*) in the xanthophyll cycle (see, e.g., Papageorgiou and Govindjee 2014); *Z* acts as a fluorescence quencher (*q*) in PSII antenna by increasing the rate constant of radiationless deactivation of the singlet excited ^{1}Chl* (i.e., k_D; see Tables 2 and 3 in the "Appendix"). Further, qE is reversed by epoxidation of *Z* to *V* by a constitutively active epoxidase (see Eqs A16 and A17 in the "Appendix"). At the same time, the contribution of Light-Harvesting Complex Stress-Related proteins (e.g., LhcSR3) to qE, which is responsible for the qE phase, and occurs in seconds, was neglected by Ebenhöh et al. (2014)

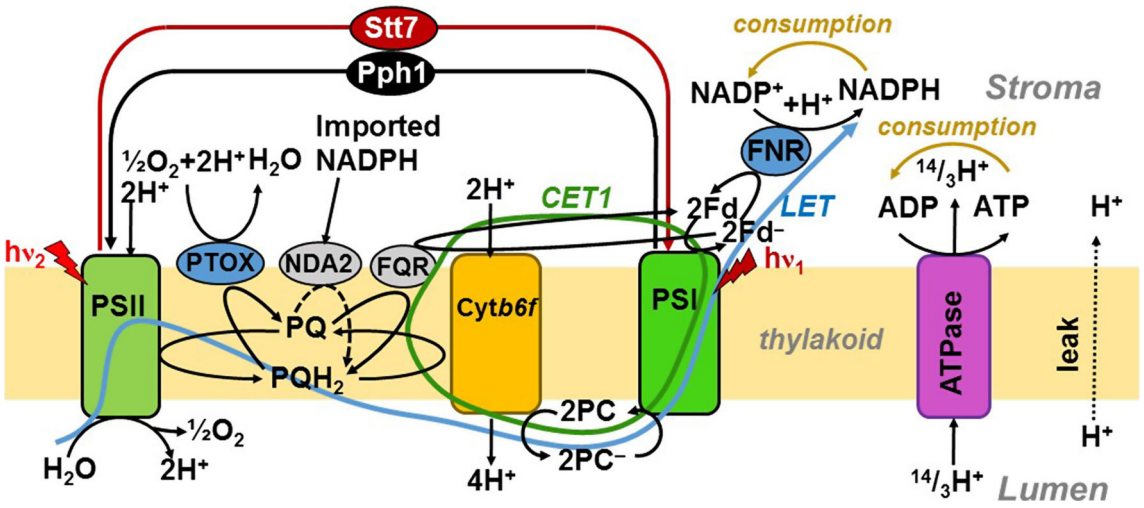

Fig. 3 Diagram of the photosynthesis model as used by Ebenhöh et al. (2014), showing the main processes involved in the short-term acclimation of the photosynthetic electron transfer chain to changing light (see explanations in the main text). *PSII and PSI*: photosystem II and I; *PQ and PQH_2*: oxidized and reduced plastoquinone; *PTOX*: plastid terminal oxidase; *NDA2*: a monomeric type-II NA(D)H dehydrogenase; *FQR*: ferredoxin:plastoquinone oxidoreductase (FQR)-dependent cyclic electron transport around PSI; *Cyt*: cytochrome; *PC*: plastocyanin; *Fd*: ferredoxin; *FNR*: Ferredoxin-$NADP^+$ oxidoreductase; *NADP*: nicotinamide adenine dinucleotide phosphate; *LET*: linear electron transport; *CET1*: cyclic electron transport around PSI; *14/3 H^+ in ATP synthesis*: the number of protons necessary for the synthesis of one ATP; *Stt7*: LHCII kinase required for the phosphorylation of mobile LHCII in *Chlamydomonas reinhardtii* that is necessary to induce state 1-to-2 transition; *Pph1*: LHCII phosphatase required for dephosphorylation of mobile LHCII that is necessary to induce the state 2-to-1 transition. ATPase refers to ATP synthase. Figure modified from Ebenhöh et al. (2014)

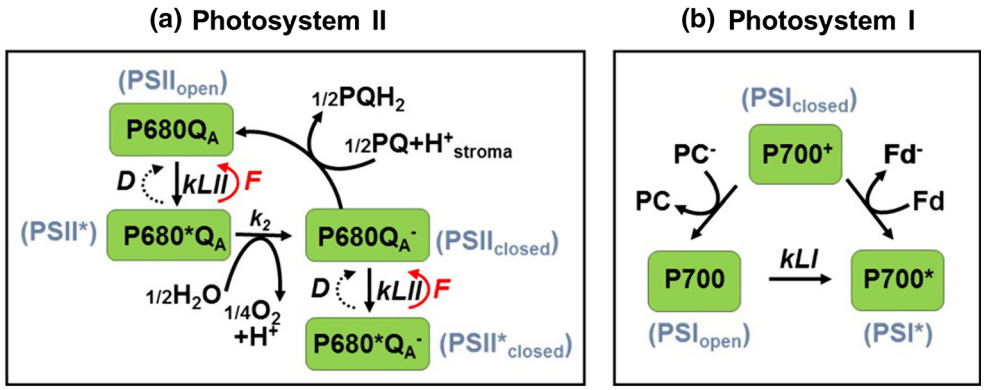

Fig. 4 Diagram of the photosystem (PS) II (**a**) and PSI (**b**) models, used by Ebenhöh et al. (2014). *P680*: PSII reaction center; Q_A: the primary plastoquinone acceptor; *PQ and* PQH_2: oxidized and reduced plastoquinone in PQ pool; *F*: Chl *a* fluorescence; *D*: radiationless dissipation of excitation energy in PSII; *kLII*: rate constant of PSII light activation; k_2: rate constant of Q_A reduction; *kLI*: rate constant of PSI light activation; *PC*: plastocyanin; *Fd*: ferredoxin. Figure modified from Ebenhöh et al. (2014)

in their model; this was because the Chlamydomonas cells used in their experiments were grown in dim light, and thus, LhcSR3 was not expressed (Peers et al. 2009).

In dealing with "*state transitions*," Ebenhöh et al. (2014) assumed that the mobile PSII antenna (mAnt) absorbed 80 % of light, as was found earlier in *C. reinhardtii* by Delosme et al. (1996). Future research must take into account a small part of mobile LHCII that may not be transferring excitation energy to either PSI or PSII (see Wlodarczyk et al. (2015)). State transitions were assumed to be triggered by the redox state of PQ pool: a reduced PQ pool will activate the kinase Stt (that phosphorylates mAnt) and induce a state 1-to-2 transition, while an oxidized PQ pool will deactivate the kinase and, due to the phosphatase Pph activity, it will induce a state 2-to-1 transition; Pph is assumed to be active all the time, but to function at a lower rate than Stt (see Eq A19 and A20 in the "Appendix").

Ebenhöh et al. (2014) used the following relationship to calculate the relative PSII fluorescence yield:

$$F_{\mathrm{PSII}}(t) = \mathrm{CSII}(t) \cdot \left[\mathrm{PSII}_{\mathrm{open}}(t) \cdot \frac{\mathrm{k_F}}{(\mathrm{k_F} + \mathrm{k_D}(t) + \mathrm{k_{Pchem}})} + \mathrm{PSII}_{\mathrm{closed}}(t) \cdot \frac{\mathrm{k_F}}{(\mathrm{k_F} + \mathrm{k_D}(t))} \right], \quad (1)$$

where, CSII(t) is the relative PSII cross section; $\mathrm{PSII}_{\mathrm{open}}$ (t) and $\mathrm{PSII}_{\mathrm{closed}}(t)$ are PSII centers with oxidized Q_A and with reduced Q_A, respectively; k_F is the fluorescence rate constant; $k_D(t)$ is the rate constant of radiationless deactivation of ^{1}Chl*; and k_{Pchem} is the photochemical rate constant (i.e., the rate constant of Q_A reduction; see Table 2 in the "Appendix"). However, in this paper, we have also considered PSI fluorescence in the calculation of the Chl *a* fluorescence yield (see Eq. A26 in the "Appendix").

The mathematical model per se includes coupled ordinary differential equations (ODEs) that were solved numerically using the software *Mathematica* (see details in the "Appendix" and in the Supplementary material); the parameters related to the reactions used in the model were taken from the literature or were adjusted as done by Ebenhöh et al. (2014) to fit experimental data (see Tables 2, 3 in the "Appendix").

Results and discussion

As mentioned above, Allorent et al. (2013), Kodru et al. (2013, 2015), and Ebenhöh et al. (2014) found that *C. reinhardtii* cells that were in state 2, after dark-adaptation, show during illumination a slow increase in Chl *a* fluorescence yield after the quasi-steady state S is reached. Experimentally, a state 1-to-2 transition can be initiated by a process that leads to the reduction of the PQ pool, for example, by switching from aerobic to anaerobic conditions in darkness. A decrease in the ATP level during anoxia is expected to induce an increase in glycolysis and an accumulation of reducing equivalents (e.g., NADPH; Bulté et al. 1990). Under these conditions, chlororespiration cannot function, and the PQ pool will be nonphotochemically reduced by NADPH via a dehydrogenase (i.e., NDA2 in *C. reinhardtii*; Mus et al. 2005; Jans et al. 2008) (see Fig. 3); this is expected to trigger a state 1-to-2 transition, and thus a CSII decrease.

Therefore, in order to simulate the slow S–M fluorescence rise in *C. reinhardtii*, we first simulated the state 1-to-2 transition during anoxia in darkness, and then we used these data to obtain Chl *a* fluorescence transient curves induced (in the presence of oxygen) after different periods of dark anoxia. Based on these simulations, we were able to establish the conditions necessary to trigger the slow S–M fluorescence rise, to study the influence of different factors on its amplitude, and to analyze the

dynamics of various variables of the model during these transients. Since *C. reinhardtii* cells grown in low light have a reduced capacity for qE-dependent quenching (Peers et al. 2009), we have neglected qE in all the simulations, with the exception of those showing the effect of qE on the S–M rise.

Mathematical simulation of the state 1-to-2 transition induced during dark anoxia

In Fig. 5a, we present results of in silico dark-adaptation of a photosynthetic sample under anoxia; we assumed that, previously, this sample had been kept in darkness in the presence of oxygen, and thus had initially an oxidized PQ pool (i.e., $PQ/PQ_{tot} = 1$) and was in state 1 (i.e., the relative PSII absorption cross section CSII = 0.8). The results of our simulations show (see Fig. 5a, panel 1) that the PQ pool is gradually being reduced nonphotochemically, via NDA2, due to changes following the inhibition of respiration (see Bulté et al. 1990); this induces a state 1-to-2 transition leading to a CSII decrease (from 0.8 to a much lower value, ~0.2). At the same time, PSII reaction centers become partially closed (Fig. 5a, panel 2), as a result of the back reaction from PQH_2 to Q_A. We note that these results are in agreement with experimental data showing an increase in the apparent F_0 in Chl *a* fluorescence transients measured after anoxia, in darkness (Haldimann and Strasser 1999).

Mathematical simulation of the slow S–M fluorescence rise

In order to simulate a Chl *a* fluorescence transient curve induced (in the presence of oxygen) after a certain period of dark-adaptation under anoxic conditions (e.g., 200, 500, 600 s; see Figs. 5, 6, 7), we used the data obtained in the in silico experiment of anoxia in darkness. Basically, we used the concentrations of the dynamic variables of the model (i.e., PSII and PSI states, PQ, PC, Fd, NADPH, ATP, H^+ in lumen, *q*, and mAnt) at the end of that specific period of anoxia in darkness, as the initial data for the numerical integration of the ODE system of the model (see "Appendix").

We found that illumination with low light (100 µmol photons m^{-2} s^{-1}) after dark anoxia can induce a state 1-to-2 transition, if the initial CSII is bigger than 0.5 (Fig. 5b), or a state 2-to-1 transition if CSII is smaller than 0.5 (Fig. 5c). Indeed, in Fig. 5b (cf. panel 1), we note that after 200 s anoxia in darkness (when the initial CSII > 0.5), the PQ pool is rapidly (in less than 1 s) reduced in light by PSII, which thus triggers a state 1-to-2 transition. During qT_{12}, however, when CSII decreases and CSI increases, the

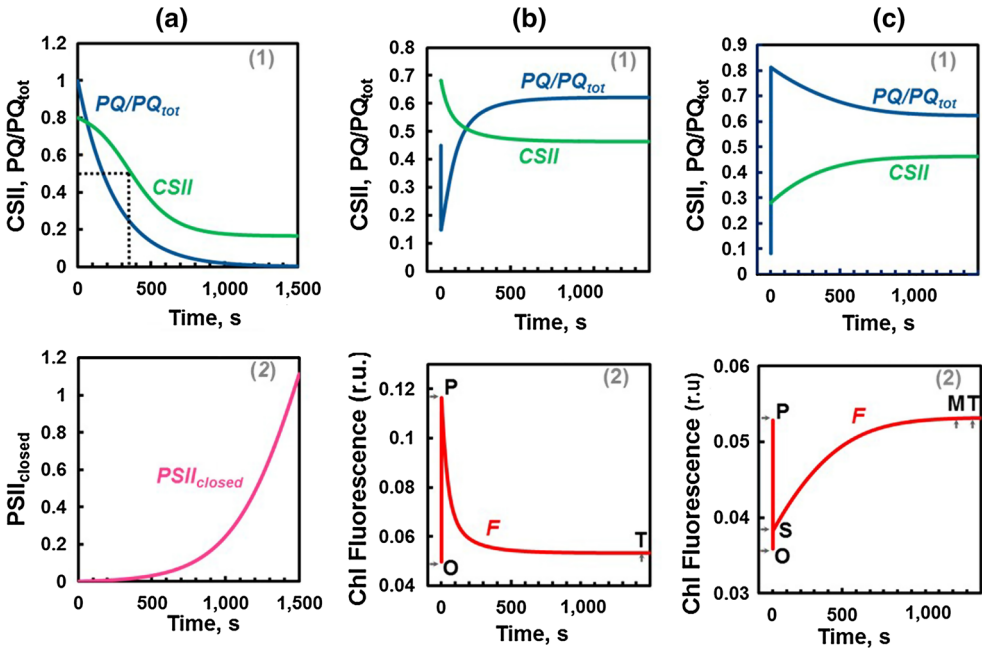

Fig. 5 In silico dark-adaptation of a photosynthetic sample in anoxic conditions (**a**) and of chlorophyll (Chl) *a* fluorescence induction under 100 µmol photons m^{-2} s^{-1} in the presence of oxygen, after 200 s (**b**) and 600 s (**c**) dark-adaptation in anoxic conditions; note that the initial relative photosystem II (PSII) absorption cross section was CSII > 0.5 in (**b**), and CSII < 0.5 in (**c**). We show the kinetics of relative plastoquinone (PQ) concentration (PQ/PQ_{tot}) and of relative PSII absorption cross section (CSII) in panels **1** (**a, b, c**); the kinetics of closed PSII reaction centers ($PSII_{closed}$) in panel **2** (**a**); and Chl *a* fluorescence (*F*) transients in panels **2** (**b, c**). These simulations are based on a modified version of a model by Ebenhöh et al. (2014)

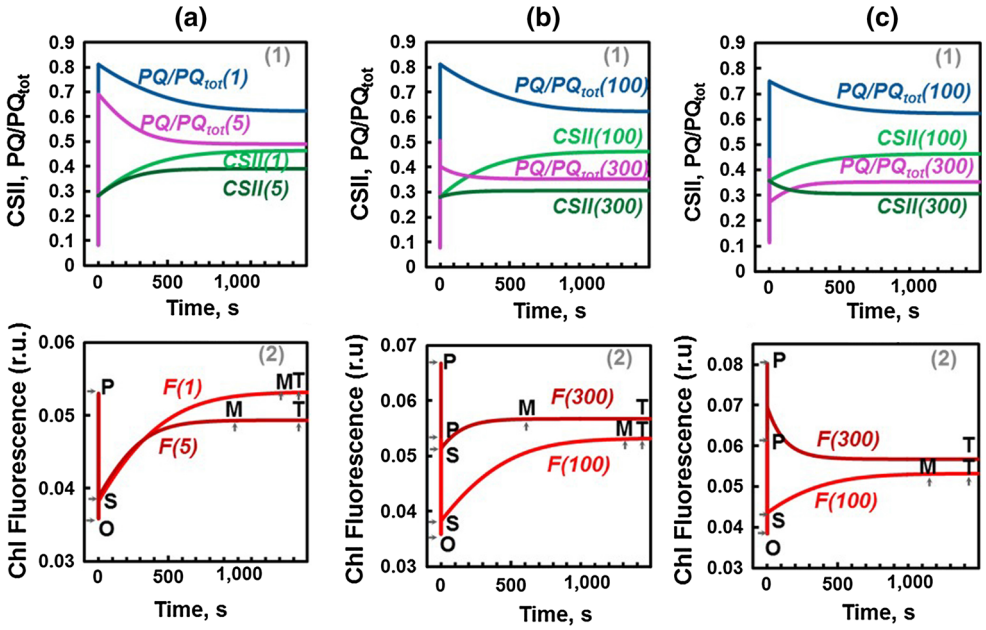

Fig. 6 In silico chlorophyll (Chl) *a* fluorescence induction after 600 s (**a**, **b**) and 500 s (**c**) of dark-adaptation in anoxic conditions, when the initial relative photosystem II absorption cross section CSII < 0.5: in (**a**), the rate constant of cyclic electron transport around photosystem I is $k_{Cyc} = 1$ or 5 s^{-1} and the illumination is 100 µmol photons m^{-2} - s^{-1}; in (**b**) and (**c**), $k_{Cyc} = 1$ s^{-1}, and the illumination is 100 or 300 µmol photons m^{-2} s^{-1}. We show the kinetics of relative plastoquinone (PQ) concentration (PQ/PQ_{tot}), and relative PSII absorption cross section (CSII) in panels **1** (**a, b**, **c**); and Chl *a* fluorescence (F) transients in panels **2** (**a, b**, **c**). These simulations are based on a modified version of a model by Ebenhöh et al. (2014)

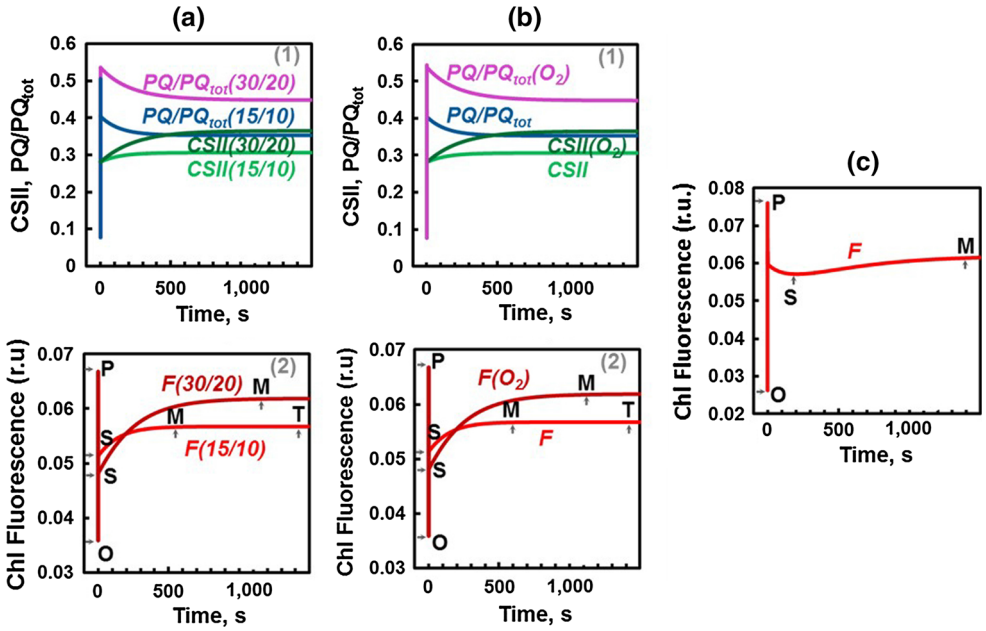

Fig. 7 In silico chlorophyll (Chl) *a* fluorescence induction under 300 µmol photons m^{-2} s^{-1}, after 600 s of dark-adaptation in anoxic conditions, when the initial relative photosystem II absorption cross section (CSII) is <0.5; in (**a**), the rate constants of ATP and NADPH consumption by the Calvin–Benson cycle (and other metabolic processes) are $k_{ATPcon} = 15$ s^{-1} and $k_{NADPHcon} = 10$ s^{-1} (labeled 15/10), or 30 and 20 s^{-1} (labeled 30/20); in (**b**), $k_{ATPcon} = 15$ s^{-1} and $k_{NADPHcon} = 10$ s^{-1}, but there is also oxygen consumption in Mehler reaction, with $k_{O_2} = 11$ s^{-1}; and in (**c**), besides state 2-to-1 transition, induction of high-energy nonphotochemical quenching qE is also assumed to take place. We show Chl *a* fluorescence (F) transients in panels **1** (**a, b**, **c**); and the kinetics of relative plastoquinone (PQ) concentration (PQ/PQ_{tot}), and relative PSII absorption cross section (CSII) in panels **2** (**a**, **b**). These simulations are based on a modified version of a model by Ebenhöh et al. (2014)

PQ pool is slowly reoxidized by PSI until it reaches a certain redox poise. Since the fluorescence yield of PSII is higher than that of PSI (Kitajima and Butler 1975; see "Appendix"), the simulation shows a fluorescence decrease to the T level (Fig. 5b, panel 2).

In the second case, after 600 s anoxia in darkness (when the initial CSII < 0.5), the PQ pool is rapidly (in less than 1 s) oxidized in light by PSI, which triggers a state 2-to-1 transition, when CSII increases and CSI decreases (Fig. 5c, panel 1); here, during qT_{21}, PQ pool is reduced by PSII. Thus, the fluorescence yield slowly increases, following the increase of CSII, generating the S–M rise (Fig. 5c, panel 2). We note that the oxidation of the PQ pool at the beginning of illumination takes place in less than one second in our simulations because the FNR and the Calvin-Benson cycle enzymes are assumed to be active in the model. Further, as expected, we found that the variation in CSII during qT_{21}, as well as in the amplitude of the S–M rise, are smaller when the initial CSII is closer to 0.5, but these increase in simulations in which longer periods of dark-adaptation in anoxic conditions are considered. However, as we will show later, several parameters of the model, from which the most important are the light intensity, the rate constants of CET1, Mehler reaction, and ATP and NADPH consumption, affect strongly the initial CSII value (i.e., the CSII threshold) at which qT_{21} is triggered.

The influence of different photosynthetic processes on the slow S–M fluorescence rise

Besides the initial value of CSII mentioned earlier, other factors may influence the amplitude of the slow S–M fluorescence rise. Since the data of Kodru et al. (2015) and our simulation results (see above) suggest that the origin of the S–M rise is a state transition (i.e., qT_{21}), and as explained earlier, state transitions are regulated by changes in the redox state of PQ pool, it follows that all processes that change the redox level of the PQ pool would affect the amplitude of the SM rise. Figure 3 shows that these processes include PSII and PSI reactions, cyclic electron transport (CET1), PQH_2 oxidation by chlororespiration, PQ reduction by NADPH, O_2 reduction by Fd^- in the Mehler reaction, and NADPH consumption in metabolic reactions.

Below, we present simulation results showing that higher rates of processes that decrease the degree of PQ pool oxidation, attained rapidly upon illumination, will lower the amplitude of the S–M rise, while higher rates of processes leading to a further PQ pool oxidation will increase the amplitude of the S–M rise. Furthermore, we also show that the presence of qE has an important impact on both the shape and the amplitude of the slow S–M fluorescence rise.

Factors that lower the amplitude of the slow S–M fluorescence rise

As shown earlier, an initial CSII < 0.5 can trigger a qT_{21}, since the PQ pool will be oxidized when PSII activity is lower compared to that of PSI. However, the relative contributions of other processes that reduce the PQ pool, such as CET1 and the reaction of PQ with NADPH (via NDA2) (see the curved arrows around PQ and PQH_2 in Fig. 3), will affect the oxidation level of the PQ pool as well as the total CSII change during the state transition, and thus the amplitude of the S–M fluorescence rise.

For example, in Fig. 6a we see that the assignment of a higher value to the rate constant of cyclic electron transport k_{Cyc} (i.e., 5 s^{-1} instead of 1 s^{-1}), under conditions that trigger a state 2-to-1 transition (i.e., initial CSII < 0.5), leads to: (1) a decrease in the degree of PQ pool oxidation reached rapidly upon illumination; (2) a lower total CSII change during qT_{21}; and (3) a smaller amplitude of the S–M fluorescence rise. Further, we also found that, as expected (Alric 2010; Joliot and Johnson 2011), when a higher CET1 rate is used in simulations, the ATP level increases, while the NADPH level decreases (results not shown).

A decrease of the S–M rise was also obtained by keeping $k_{Cyc} = 1$, but by increasing light intensity from 100 to 300 μmol photons m^{-2} s^{-1} (Fig. 6b). However, we found that, when the duration of the dark-adaptation, under anoxic conditions, is closer to the threshold at which qT_{21} occurs (e.g., 500 s, in Fig.6c, instead of 600 s, in Fig. 6b), a similar increase in light intensity induces a qT_{12} instead of qT_{21} (see Fig. 6c). These results are in agreement with experimental results (see, e.g., data on *Chlorella* by Papageorgiou and Govindjee 1968a), which show that the slow S–M fluorescence rise is relatively larger at lower exciting light intensities; and, this was the main reason why we used in simulations only low or medium light intensity, and not saturating light, especially since we have examined samples with a relative low degree of qT_{12} induced during dark anoxia.

Factors that increase the amplitude of the slow S–M fluorescence rise

As mentioned earlier, the Calvin–Benson cycle and other metabolic processes have been considered only implicitly in the photosynthesis model used here. It is well known that, until saturation takes place, consumption of both ATP and NADPH increases when the light intensity is increased. Here we show that an increase in the rate constants of ATP and NADPH consumption, under conditions that trigger a qT_{21} (i.e., initial CSII < 0.5), will also increase the

amplitude of the slow S–M fluorescence rise. From the simulated curves presented in Fig. 7a, we see that, at 300 μmol photons m^{-2} s^{-1}, an increase in the rate constant of ATP consumption from 15 to 30 s^{-1}, and in that of NADPH consumption from 10 to 20 s^{-1}, leads to: (1) a greater degree of PQ pool oxidation at the beginning of illumination; (2) a larger variation of CSII during qT_{21}; and (3) to a higher amplitude of the S–M rise. However, for higher rate constants of ATP and NADPH consumption, there is a saturation effect, and the amplitude of the S–M rise increases only slightly (results not shown).

Another process that increases the amplitude of the S–M rise is the Mehler reaction (see Fig. 7b, panel 2), an alternate electron sink for PSI, in which Fd^- reduces O_2 (Mehler 1951; Kono et al. 2014; Tikhonov 2015). Ebenhöh et al. (2014) did not consider this reaction in their model; however, we have used the following expression to calculate its rate (see Tikhonov and Vershubskii 2014):

$$v_{O_2} = k_{O_2} \cdot O_2^{ex} \cdot (Fd_{tot} - Fd), \quad (2)$$

where k_{O_2} is the rate constant of Mehler reaction; O_2^{ext} is the external O_2 concentration; Fd is the oxidized ferredoxin concentration; and Fd_{tot} is the Fd pool size (see also Tables 1 and 2 in the "Appendix"). Besides the increase in the amplitude of the S–M rise, the inclusion in the model of the Mehler reaction leads to a decrease in PQ pool reduction, similar to that calculated after an increase in ATP and NADPH consumption (as shown in Figs. 7a, and 7b), emphasizing its role in the reduction of the excitation pressure.

The effect of qE on the slow S–M fluorescence rise

Here, we discuss our results obtained when not only state transitions but also the high-energy nonphotochemical quenching of singlet excited Chl *a* in PSII antenna (qE) has been included in the simulation of Chl *a* fluorescence transients under conditions that allow the induction of qT_{21} (i.e., initial CSII < 0.5). We found that, depending on the rate constant of violaxanthin de-epoxidation to zeaxanthin (i.e., kNh; see Eq A16 in the "Appendix"), involved in qE, and that of LHCII dephosphorylation (i.e., kPph; see Eq A19 in "Appendix"), involved in qT, the fluorescence curves either: (1) decrease to the T level, without a visible S–M rise, if qE is dominant (not shown), or (2) show an S–M rise, after an initial fluorescence decrease from P to a steady state S, if qT is high (see Fig. 7c). In the second case, the S level, as well as the amplitude of the S–M rise, is lowered compared to the fluorescence induction curves simulated only in the presence of qT.

By including qE in the simulation of Chl *a* fluorescence transients, we had thought that we would simulate the M–T decay, and decrease the time at which the M level is reached, but the results in Fig. 7c suggest that other processes must be also involved in controlling this phase, or that qE (as described in Ebenhöh et al. 2014) must be redefined. However, these results, although incomplete, provide us an impetus to go forward to find the right model to simulate the entire SMT phase.

Conclusions

In this paper, we have simulated Chl *a* fluorescence induction curves in continuous light, using a slightly modified version of the model of Ebenhöh et al. (2014) (see the "Appendix"), in which the short-term regulation processes of high-energy NPQ quenching (qE) and state transitions (qT) are both included. Our results show that a slow (hundreds of seconds) S–M fluorescence rise can be mathematically simulated only if the photosynthetic system is initially in state 2, when PSII has initially a cross section (CSII) smaller than that of PSI (i.e., CSII < 0.5); for samples initially in state 1 (i.e., CSII > 0.5) the simulated Chl *a* fluorescence decreases continuously from P to the T level (see Fig. 5b).

Under conditions that favor a qT_{21}, the S–M rise is less visible when the initial CSII is closer to 0.5, but it becomes significant at lower CSII values. Our results suggest that photosynthetic organisms are very sensitive to differences between the relative absorption cross sections of the two photosystems, as these lead to large changes in the redox state of PQ pool, which consequently induce(s) state transitions during which the PQ pool changes to have a new redox poise (see, e.g., Fig. 5b, and Fig. 5c).

However, since state transitions in higher plants involve relatively fewer mobile LHCII trimers than in green algae (Rochaix 2014), it is possible that conditions that allow the generation of a slow S–M rise in higher plants cannot be generally achieved. Therefore, since the small S–M rise observed in higher plants appears early (i.e., after $\sim$10 s; see Fig. 1a), it is possible that this may have causes other than a state 2-to-1 transition. Further research is needed to understand the S–M rise in higher plants since, in specific cases of abiotic or biotic stress, a slower and larger S–M rise than that shown in Fig. 1a was observed. For example, Pandey and Gopal (2012) found that wheat plants treated with dimethoate (i.e., O,O-dimethyl S-methylcarbamoylmethyl phosphorodithioate) show a relatively high S–M fluorescence rise, where the M level is reached after $\sim$100 s. Further, K. Mishra, A. Mishra and Govindjee (personal communication, 2015) have shown that freezing temperatures also induce significantly large S–M rise in *Arabidopsis thaliana*, where the level M is reached in tens of seconds.

Moreover, we found that the initial CSII threshold, over which the fluorescence transients show a slow S–M rise, and the amplitude of the S–M rise depend on factors and processes that affect the redox state of PQ pool: (1) those that reduce further the PQ pool (e.g., higher rate of CET1 and light intensity) increase the CSII threshold and lower the S–M rise amplitude (see Fig. 6a, and Fig. 6b); and (2) those that oxidize the PQ pool (e.g., higher rates of the Calvin–Benson cycle and the presence of Mehler reaction) lower the CSII threshold and increase the S–M rise amplitude (Fig. 7a, Fig. 7b).

Finally, results of our simulations, in the presence of both qE and qT_{21}, show that either the slow S–M fluorescence rise is missing (i.e., the fluorescence decreases continuously from the P to T level) or has a lower amplitude (Fig. 7c), depending on the initial conditions and the parameters used in the relationships that define the qE and state transitions in the model (see "Appendix").

We show in this paper that the origin of the slow S–M rise in *C. reinhardtii* is a state 2-to-1 transition; further, we have found the basic conditions that allow its formation and influence its amplitude, which was, indeed, our main goal. On the other hand, the experimental Chl *a* fluorescence induction curves could not be fitted well enough by curves simulated using the photosynthesis model and parameters of Ebenhöh et al. (2014), with the minor modifications used (see "Appendix"): the fast O–P rise was not multiphasic (due to the use of minimal PSII model; see Fig. 4a), the fluorescence decrease from P to S was slower than that observed experimentally (since only the zeaxanthin quenching was considered in the definition of qE), the maximum M was reached after a much longer time, and the characteristic M–T decrease was missing. In order to understand the complete OJIPS(M)T transient, and to precisely fit the experimental curves, we plan to modify and extend the current model; this would be especially relevant for those parts of the model related to PSII, the kinetics of qE and qT, as well as the consumption of ATP and NADPH during the Calvin–Benson cycle and other metabolic reactions.

Acknowledgments We are highly grateful to Prof. Oliver Ebenhöh and Anna Matuszyńska for allowing access to the source code of their photosynthesis model, for their suggestions on the manuscript, especially on the Supplementary material, and for verifying the reproducibility of our data. We also thank our reviewers for their very useful comments, which have helped us to improve the manuscript. Govindjee thanks the Department of Plant Biology (Professor James Dalling, and his staff), Department of Biochemistry (Professor Susan Martinis and her staff), and the Office of Information Technology, Life Sciences (Director Jeff Haas, and his staff) of the University of Illinois at Urbana-Champaign (UIUC) for support during this work.

Appendix

The photosynthesis model of Ebenhöh et al. (2014)

The photosynthesis model of Ebenhöh et al. (2014) has been discussed in detail in the supplementary material of their paper, and thus, we present here only its basics, as well as the features that we have adjusted or added in the simulations presented in this paper. As explained in the main text, this mathematical model is centered on processes related to the light phase of photosynthesis as shown in Fig. 3, and its core consists of a system of coupled ordinary differential equations (ODE) describing the kinetics of the main components participating in these processes, which represent the dynamic variables of the model.

For an easy understanding of the ODE system, we provide first the meaning of the symbols used. In what follows, the labels for the dynamic variables are pq, for the oxidized plastoquinone (PQ); pc, for the oxidized plastocyanin (PC); fd, for the oxidized ferredoxin (Fd); nh, for the reduced dinucleotide adenine phosphate (NADPH); atp, for ATP; hi, for the H^+ concentration in lumen; mAnt, for the fraction of the total cross section represented by non-phosphorylated mobile antenna associated with PSII; q, for the relative PSII antenna quencher concentration; b_0, for the [P680 Q_A] state of PSII; b_1, for the [P680* Q_A] state of PSII; b_c, for the [P680 Q_A^-] state of PSII; b_3, for the [P680* Q_A^-] state of PSII; y_0, for the [P700] state of PSI; y_1, for the [P700*] state of PSI; and y_c, for the [$P700^+$] state of PSI. The mathematical expressions of all the rates of processes considered in the model (e.g., v_{PSII}, v_{b6f}, and v_{Cyc}) are shown in Table 1; these are functions of dynamic variables, as well as external constants and parameters of the model, and were derived considering the kinetics of the reactions taking place in each process (see Fig. 3). The values of constant parameters used in this model are mainly from the literature, and are given in Table 2. Here we note that, due to the simplicity of the PSII model used by Ebenhöh et al. (2014), we had to assign a higher value to the equilibrium constant of the PQ reduction by Q_A^- (see Table 2), in order to improve the fit of our simulated Chl *a* fluorescence induction curves with experimental data.

Further, a number of parameters were defined as functions of different dynamic variables, and thus are time dependent; these time-dependent parameters are presented separately in Table 3.

The ODE system is:

$$\frac{d(pq)}{dt} = -(1/2)v_{PSII} + v_{b6f} - v_{Cyc} + v_{PTOX} - v_{NDH} \quad (A1)$$

Table 1 Mathematical expressions of all the rates of processes considered in the ODE system (see also Ebenhöh et al. 2014 in this paper)

Process	Rate of the process
PSII e^- transfer	$v_{PSII} = k_{Pchem} \cdot b_1$
PSI e^- transfer	$v_{PSI} = k_{LI} \cdot y_0$
Chlororespiration	$v_{PTOX} = k_{PTOX} \cdot (pq_{tot} - pq) \cdot O_2^{ext}$
PQ reduction by NADPH	$v_{NDH} = k_{NDH} \cdot pq$
Cyt *b6f* e^- transfer	$v_{b6f} = \mathrm{Max}[k_{b6f} \cdot ((pq_{tot} - pq) \cdot pc^2 - pq \cdot (pc_{tot} - pc)^2 / k_{eqb6f}),\ v_{b6fmin}]$
PQ reduction by Fd^-	$v_{Cyc} = k_{Cyc} \cdot (fd_{tot} - fd)^2 \cdot pq$
O_2 reduction by Fd^-	$v_{O_2} = k_{O_2} \cdot O_2^{ext} \cdot (fd_{tot} - fd)$
FNR e^- transfer	$v_{FNR} = v_{FNRmax} \cdot \left(fdred^2 \cdot nadp - fdox^2 \cdot nadph / k_{eqFNR}\right) / \left(\left(1 + fdred + fdred^2\right) \cdot (1 + nadp) + \left(1 + fdox + fdox^2\right) \cdot (1 + nadph) - 1\right)$
H^+ leak across membrane	$v_{Leak} = k_{Leak} \cdot (hi - ho)$
ATP synthesis	$v_{ATPsyn} = k_{ATPsyn} \cdot (ap_{tot} - atp - atp / k_{eqATPsyn})$
ATP consumption	$v_{ATPcon} = k_{ATPcon} \cdot atp$
NADPH consumption	$v_{NADPHcon} = k_{NADPHcon} \cdot nh$
State 1-to-2 transition	$v_{1\ to\ 2} = k_{Stt} \cdot (1/(1 + ((pq/pq_{tot})/k_{MST})^{nST})) \cdot mAnt$
State 2-to-1 transition	$v_{2\ to\ 1} = k_{Pph} \cdot (1 - mAnt)$
V de-epoxidation to *Z*	$v_{deep} = k_{Nh} \cdot (1 - q) \cdot (hi^{nQ} / (hi^{nQ} + k_{MQ}^{nQ}))$
Z epoxidation to *V*	$v_{epox} = k_{Nr} * q$

The values of the constant parameters used in simulations are given in Table 2, and the time-dependent parameters in Table 3

$$\frac{d(pc)}{dt} = -2v_{b6f} + v_{PSI} \quad (A2)$$

$$\frac{d(fd)}{dt} = -v_{PSI} + 2v_{FNR} + 2v_{Cyc}(+v_{O_2}) \quad (A3)$$

$$\frac{d(nh)}{dt} = v_{FNR} - v_{NADPHcon} \quad (A4)$$

$$\frac{d(atp)}{dt} = v_{ATPsyn} - v_{ATPcon} \quad (A5)$$

$$\frac{d(hi)}{dt} = \frac{1}{b_H}\left(v_{PSII} + 4v_{b6f} - hpr \cdot v_{ATPsyn} - v_{Leak}\right) \quad (A6)$$

$$\frac{d(mAnt)}{dt} = -v_{1\ to\ 2} + v_{2\ to\ 1} \quad (A7)$$

$$\frac{d(q)}{dt} = v_{deep} - v_{epox} \quad (A8)$$

$$\frac{d(b_0)}{dt} = -\left[k_{LII} + \frac{k_{PQred}}{k_{eqPQred}} \cdot (pq_{tot} - pq)\right] \cdot b_0 + (k_D + k_F) \cdot b_1 + k_{PQred} \cdot pq \cdot b_c\,(= 0) \quad (A9)$$

$$\frac{d(b_1)}{dt} = k_{LII} \cdot b_0 - (k_D + k_F + k_{Pchem}) \cdot b_1 (= 0) \quad (A10)$$

$$\frac{d(b_3)}{dt} = k_{LII} \cdot b_c - (k_D + k_F) \cdot b_3 (= 0) \quad (A11)$$

$$b_c = psII^{tot} - b_0 - b_1 - b_3 \quad (A12)$$

$$\frac{d(y_0)}{dt} = \left(-k_{LI} - \frac{k_{PCox}}{k_{eqPCP700}} \cdot pc\right) \cdot y_0 + k_{PCox} \cdot (pc_{tot} - pc) \cdot y_c (= 0) \quad (A13)$$

$$\frac{d(y_1)}{dt} = k_{LI} \cdot y_0 - k_{FDred} \cdot fd \cdot y_1 + \frac{k_{Fdred}}{k_{eqFAFd}} \cdot (fd_{tot} - fd) \cdot y_c (= 0) \quad (A14)$$

$$y_c = psI_{tot} - y_0 - y_1. \quad (A15)$$

In each of the first 8 differential equations (Eqs. A1–A8), the variation in time of the concentration of one variable (i.e., its derivative) was equated with the algebraic sum of the rates of all processes in which this variable is involved, considering also the respective stoichiometry: a positive sign was assigned to the rate of processes that generate the variable, while a negative sign was assigned to the rates of processes in which the variable is consumed. For example, based on the reaction scheme shown in Fig. 3, the change in time of the concentration of PC (see Eq. A2) is equal to the rate of PSI (i.e., v_{PSI}) minus the rate of Cyt *b6f* (i.e., v_{b6f}). Also, we note that in Eq. A3, related to Fd, we added the rate of Mehler reaction, but only in the simulations that show the effect of this alternative electron flow on the amplitude of the slow S–M fluorescence rise.

Table 2 Values of the constant parameters used in simulations. Most of these parameters have the same values as those used by Ebenhöh et al. (2014; Table S1), but if different, the original value is also given in parenthesis

Parameter	Meaning	Value	Ref.
Pool sizes			
$psII_{tot}$	PSII total	2.5 mmol (mol Chl)$^{-1}$	Schöttler et al. (2004)
psI_{tot}	PSI total	2.5 mmol (mol Chl)$^{-1}$	Schöttler et al. (2004)
pq_{tot}	PQ pool size	17.5 mmol (mol Chl)$^{-1}$	Kirchhoff et al. (2002)
pc_{tot}	PC pool size	4 mmol (mol Chl)$^{-1}$	Böhme (1978)
fd_{tot}	Fd pool size	5 mmol (mol Chl)$^{-1}$	Böhme (1978)
$nadp_{tot}$	NADPH pool size	25 mmol (mol Chl)$^{-1}$	Heineke et al. (1991)
ap_{tot}	ATP pool size	60 mmol (mol Chl)$^{-1}$	Heineke et al. (1991)
Rate constants of different reactions			
k_{Pchem}	Q_A reduction	2×10^9 s^{-1}; ($5{\cdot}10^9$)	Mar et al. (1972)
k_{PQred}	PQ reduction by Q_A^-	100 mmol^{-1} (mol Chl) s^{-1}; (250)	de Wijn and van Gorkom (2001)
k_{PTOX}	O_2 reduction by PQH_2	0.01 mmol^{-1} (mol Chl) s^{-1}	Fitted to inter-flash F_S-dynamics in aerobic conditions by Ebenhöh et al. (2014)
k_{NDH}	PQ reduction by NADPH	0.004 s^{-1} (0.002)	Fitted to inter-flash F_S-dynamics in anaerobic conditions by Ebenhöh et al. (2014)
k_{b6f}	PQH_2 oxidation by Cyt *b6f*	2.5 mmol^{-2} (mol Chl)^2 s^{-1}	Finazzi et al. (1999)
v_{b6fmin}	Minimum Cyt *b6f* rate	−2.5 mmol (mol Chl)$^{-1}$ s^{-1}	Ad hoc estimate by Ebenhöh et al. (2014), to avoid strong reverse currents
k_{PCox}	PC^- oxidation by $P700^+$	2500 mmol^{-1}(mol Chl)s^{-1}	Farah et al. (1995)
k_{Fdred}	Fd reduction by F_A^-	$2.5{\cdot}10^5$ mmol^{-1}(mol Chl) s^{-1}	Sétif and Bottin (1994)
k_{Cyc}	CET1 (PQ reduction by Fd^-)	1 mmol^{-2} (mol Chl)^2 s^{-1}	Ad hoc estimate by Ebenhöh et al. (2014)
k_{O_2}	O_2 reduction by Fd^-	11 s^{-1}	Tikhonov and Vershubskii (2014)
v_{FNRmax}	Maximum FNR rate	1500 mmol (mol Chl)$^{-1}$s^{-1}	Carrillo and Ceccarelli (2003)
$k_{NADPHcon}$	NADPH consumption	10 s^{-1} (15)	Fitted by Ebenhöh et al. (2014) to yield a reasonable NADPH:NADP ratio
k_{ATPcon}	ATP consumption	15 s^{-1} (10)	Fitted by Ebenhöh et al. (2014) to yield a reasonable ATP:ADP ratio
k_{ATPsyn}	ATP synthesis	20 s^{-1}	Fitted to allow for a CO_2 fixation rate of 500 µmol reduced CO_2 (µmol Chl)$^{-1}$h^{-1}
k_{Leak}	H^+ leak through thylakoid membrane	0.01 s^{-1}	Ad hoc estimate by Ebenhöh et al. (2014)
k_F	Chl fluorescence emission	$6.25{\cdot}10^7$ s^{-1}	Zaks et al. (2012)
k_{Dconst}	Basic PSII radiationless excitation energy dissipation	$5{\cdot}10^8$ s^{-1}	Mar et al. (1972)
k_{Ddyn}	PSII radiationless excitation energy dissipation in the presence of quenchers	$5{\cdot}10^9$ s^{-1}	Zaks et al. (2012)
k_{Stt}	LHCII phosphorylation by Stt	0.005 s^{-1}; (0.0035)	Fitted to F_M-dynamics by Ebenhöh et al. (2014)
k_{Pph}	LHCII dephosphorylation by Pph	0.0013 s^{-1}	Fitted to F_M-dynamics by Ebenhöh et al. (2014)
k_{Nh} (k_{deep})	V de-epoxidation to Z	0.05 s^{-1}	Pfündel and Dilley (1993)
k_{Nr} (k_{epox})	Z epoxidation to V	0.004 s^{-1}	Pfündel and Dilley (1993)
Michaelis constants			
k_{MFNRFd}	Reaction of FNR with Fd^-	1.56 mmol (mol Chl)$^{-1}$	Aliverti et al. (1990)
k_{MFNRNH}	Reaction of FNR with $NADP^+$	0.22 mmol (mol Chl)$^{-1}$	Aliverti et al. (2004)
k_{MST}	For qT; influences the PQ redox poise	0.3 (0.2)	Estimated by Ebenhöh et al. (2014) to yield a PQ redox poise of ≈1:1
k_{MQ}	For qE	Corresponding to pH 5.8	Pfündel and Dilley (1993)

Table 2 continued

Parameter	Meaning	Value	Ref.
Standard redox potentials of some electron transport components			
e_{QA}	$E^0(Q_A/Q_A^-)$	−0.140 V	Allakhverdiev et al. (2011)
e_{PQ}	$E^0(PQ/PQH_2)$	0.082 V	Okayama (1976), Antal et al. (2013)
e_{Cyt}	E^0(cytf)	0.350 V	Antal et al. (2013)
e_{PC}	$E^0(PC/PC^-)$	0.380 V	Suzuki et al. (1987)
e_{P700}	$E^0(P700^+/P700)$	0.480 V	Witt et al. (2003)
e_{FA}	$E^0(F_A/F_A^-)$	−0.550 V	Evans and Heathcote (1980)
e_{Fd}	$E^0(Fd/Fd^-)$	−0.430 V	Cammack et al. (1977)
e_{NADP}	$E^0(NADP^+/NADPH)$	−0.113 V	Nicholls and Ferguson (1997)
Equilibrium constants calculated using standard redox potentials			
$k_{eqPQred}$	For PQ reaction with Q_A^-	500; (∼13)	
k_{eqCyc}	For CET1	9.20753×10^{10}	
$k_{eqCytfPC}$	For PC reaction with Cyt f^-	3.2	
k_{eqFAFd}	For Fd reaction with F_A^-	108	
$k_{eqPCP700}$	For PC^- reaction with $P700^+$	49.5	
k_{eqNDH}	For PQ reaction with NADPH	1.055×10^8	
k_{eqFNR}	For FNR	873	
Other constants used in simulations			
Chl content	Chl concentration per m^2 membrane	350×10^{-6} mol m^{-2}	Laisk et al. (2006)
V_{lumen}	Lumen volume	0.0014 l m^{-2}	Laisk et al. (2006)
V_{stroma}	Stroma volume	0.0112 l m^{-2}	Laisk et al. (2006)
pfd	Photon flux density (PFD)	(μmol photons m^{-2} s^{-1})	
csIst	Static PSI relative absorption CS	0.2	Drop et al. (2011)
csIIst	Static PSII relative absorption CS	0.0	Drop et al. (2011)
pHo	pH in stroma	7.8	
ho	H^+ concentration in stroma	0.0004953 mmol (mol Chl)$^{-1}$	
hpr	Ratio H^+/ATP synthesized	14/3	Seelert et al. (2000)
pi	Used for ATP synthesis	0.01 mM	Usuda (1988)
bH	Proton buffer in the lumen	100	Laisk et al. (2006)
nQ	Hill coefficient (used for qE)	5	Pfündel and Dilley (1993)
nST	Hill coefficient (used for qT)	2	Ebenhöh et al. (2011)
O_2^{ext}	External O_2 concentration	8 mmol (mol Chl)$^{-1}$; 0 in anoxic conditions	
dG^0_{ATP}, (ΔG^0_{ATP})	Standard Gibbs free energy change for one ATP molecule	30.6 kJ mol^{-1}/RT	Rosing and Slater (1972)
cF	Faraday constant (F)	96.485	
cR	Universal gas constant (R)	8.3×10^{-3}	
tAbs	Absolute temperature (T), for 25 °C	298 K	

The last 7 equations (Eqs. A9–A15) apply to PSII and PSI states, and were established based on the reactions shown in the simplified schemes of PSII and PSI (see Fig. 4a, and Fig. 4b), by assuming that they proceed according to a mass-action kinetic law. The equations A9–A11 describe the dynamics of PSII states (b_0, b_1 and b_3), while the equations A13 and A14 describe those of PSI states y_0 and y_1; we note that the algebraic equations A12 and A15 show the stoichiometric relationship between the states of PSII and PSI and allow us to calculate the dynamics of b_c and y_c. The definitions given by Ebenhöh et al. (2014) for the relative absorption cross sections (CSII

Table 3 Mathematical expressions of time-dependent parameters used in simulations (see also Ebenhöh et al. 2014)

Parameter and its meaning	Expression
csII, PSII relative absorption cross section	$csII = csIIst + mAnt\cdot(1 - csIst - csIIst)$
csI, PSI relative absorption cross section	$csI = csIst + (1 - mAnt)\cdot(1 - csIst - csIIst)$
k_{LII}, rate constant of PSII light activation	$k_{LII} = cPFD\cdot csII\cdot pfd$
k_{LI}, rate constant of PSI light activation	$k_{LI} = cPFD^*(1 - csII)\cdot pfd$
k_D, rate constant of radiationless dissipation of the excitation energy in PSII	$k_D = k_{Dconst} + k_{Ddyn}\cdot q$
fdox, normalized concentration of Fd	$fdox = fd/k_{MFNRFd}$
fdred, normalized concentration of Fd^-	$fdred = (fd_{tot} - fd)/k_{MFNRFd}$
nadp, normalized concentration of $NADP^+$	$nadp = (nadp_{tot} - nh)/k_{MFNRNH}$
nadph, normalized concentration of NADPH	$nadph = nh/k_{MFNRNH}$
pHi, pH in lumen	$pHi = -\ln(2.5 \times 10^{-4}\cdot hi)/\ln(10)$
dG_{ATPsyn}, standard Gibbs free energy change of ATP synthesis (i.e., ΔG^0_{ATPsyn})	$dG_{ATPsyn} = dG^0_{ATP} - \ln(10)\cdot cR\cdot tAbs\cdot hpr\cdot(pHo - pHi)$
$k_{eqATPsyn}$, equilibrium constant of ATP synthesis	$k_{eqATPsyn} = pi\cdot\exp(-dG_{ATPsyn}/cR\cdot tAbs)$
dGb6f, standard Gibbs free energy change of Cyt *b6f* (i.e., ΔG^0_{Cytb6f})	$dG_{b6f} = 2e_{PQ}\cdot cF - 2\ln(10)\cdot cR\cdot tAbs\cdot pHi - 2\cdot e_{PC}\cdot cF + 2\ln(10)\cdot cR\cdot tAbs\cdot(pHo - pHi)$
k_{eqb6f}, equilibrium constant of Cyt *b6f*	$k_{eqb6f} = \exp(-dG_{b6f}/cR\cdot tAbs)$
*f*2, Chl *a* fluorescence from PSII	$f2 = csII\cdot[b_0\cdot k_F/(k_D + k_F + k_{Pchem}) + b_c\cdot k_F/(k_D + k_F)]$

and CSI) and the light activation rates of the two photosystems (k_{LII} and k_{LI}), as well as the rate constant of radiationless excitation energy dissipation in PSII antenna (k_D) are shown in Table 3, since these are time-dependent parameters in this model.

In order to keep their photosynthesis model as simple as possible, Ebenhöh et al. (2014) had used, in their simulations, the standard quasi-steady-state hypothesis, in which the internal states of PSII and PSI were assumed to be approximately in steady state; mathematically, this is achieved by equating all the derivatives of PSII and PSI states to zero (see parenthesis at the end of Eqs. A9–A11, A13, A14). This simplification is justified for the simulation of fluorescence quenching dynamics, in which the fluorescence data are mainly related to the steady-state phase of photosynthesis, as the electron flow within the photosystems is much faster than the electron transfer between the complexes of the transport chain. However, in our simulations of Chl *a* fluorescence transients, measured under continuous illumination, we did not use this simplification, since it is not appropriate for the fast part of the fluorescence induction curves.

As mentioned earlier, all the rates of processes involved in the first 8 equations of the ODE system are defined in Table 1. Below, we discuss only the model blocks related to qE and qT, defined by Ebenhöh et al. (2014), while the readers interested in other reactions should consult the Supplementary material of Ebenhöh et al. (2014).

The qE in this model is assumed to be triggered by low lumenal pH, which activates the de-epoxidation of *V* to *Z* in the xanthophyll cycle (Ebenhöh et al. 2011; Zaks et al. 2012; Papageorgiou and Govindjee 2014); this reaction is reversed by the epoxidation of *Z* to *V* by a constitutively active epoxidase. The activation dynamics of qE, corresponding to the process of de-epoxidation of violaxanthin to zeaxanthin, has been described by a Hill-type equation (Eq. A16; Pfündel and Dilley 1993), while the deactivation process corresponding to the epoxidation of zeaxanthin back to violaxanthin has been modeled using a first-order mass-action kinetics (Eq. A17):

$$v_{deep} = k_{Nh}\cdot(1 - q)\cdot\frac{hi^{nQ}}{\left(hi^{nQ} + k_{MQ}^{nQ}\right)} \tag{A16}$$

$$v_{epox} = k_{Nr}\cdot q, \tag{A17}$$

where (see also Table 2), the dynamic variable q is the relative concentration of the quencher (i.e., zeaxanthin; see above), which takes values between 0 and 1; k_{Nh} and k_{Nr} are the rate constants of de-epoxidation and epoxidation reactions; nQ is the Hill coefficient; and k_{MQ} is the Michaelis constant, corresponding to a switch point at pH 5.8.

Further, without an explicit description of the mechanism(s) involved, Ebenhöh et al. (2014) assumed that an increase in q enhances the de-excitation of ^{1}Chl* as heat in PSII antenna by increasing (linearly, for simplicity) the rate constant of the radiationless dissipation of the excitation energy in PSII, k_D (see Table 3):

$$k_D = k_{Dconst} + k_{Ddyn}\cdot q, \tag{A18}$$

where, k_{Dconst} is the basic PSII radiationless excitation energy dissipation; and k_{Ddyn} is the PSII radiationless excitation energy dissipation in the presence of quenchers (which is bigger than k_{Dconst}, see Table 2).

State transitions were modeled using the simplifying assumption that, after phosphorylation of the PSII mobile antenna (mAnt) by the kinase Stt7, these directly relocate to PSI, and that phosphorylated mAnt directly re-associate with PSII after their dephosphorylation by Pph1. Further, Stt7 is assumed to be regulated by the redox state of PQ pool, a reduced PQ pool activating the kinase, and an oxidized PQ pool inactivating it; on the other hand, Pph1 is considered to be constitutively active. In this model, Stt7 activity is described by a Hill-type equation with moderate cooperativity (i.e., the Hill coefficient $n = 2$; see also Tables 1 and 2):

$$v_{1\text{ to }2} = k_{\mathrm{Stt}} \cdot \left[1 - \frac{\left(\frac{\mathrm{pq}/\mathrm{pq}_{\mathrm{tot}}}{k_{\mathrm{MST}}}\right)^{\mathrm{nST}}}{1 + \left(\frac{\mathrm{pq}/\mathrm{pq}_{\mathrm{tot}}}{k_{\mathrm{MST}}}\right)^{\mathrm{nST}}}\right] \cdot \mathrm{mAnt} \quad \text{(A19)}$$

$$v_{2\text{ to }1} = k_{\mathrm{Pph}} \cdot (1 - \mathrm{mAnt}), \quad \text{(A20)}$$

where, k_{Stt} and k_{Pph} are the rate constants of Stt7 and Pph1, respectively; mAnt is the PSII mobile antenna; pq is oxidized PQ; $\mathrm{pq}_{\mathrm{tot}}$ is the PQ pool size ($\mathrm{PQ}_{\mathrm{tot}}$); k_{MST} is the Michaelis constant; and nST is the Hill coefficient.

The relative absorption cross sections of PSII and PSI (labeled as csII and csI, respectively) are assumed to change during the state transition according to the following formula (see also Table 3):

$$\mathrm{csII} = \mathrm{csIIst} + \mathrm{mAnt} \cdot (1 - \mathrm{csIst} - \mathrm{csIIst}) \quad \text{(A21)}$$

$$\mathrm{csI} = \mathrm{csIst} + (1 - \mathrm{mAnt}) \cdot (1 - \mathrm{csIst} - \mathrm{csIIst}), \quad \text{(A22)}$$

where, csIIst and csIst are antenna fixed to PSII and PSI, respectively. However, Wlodarczyk et al. (2015) have shown that only ~2/3 of the total mobile LHCII antenna transfer energy to PSI in state 2, while ~1/3 of these form a quenched component, and do not transfer energy to PSI or to PSII. Although we used in this paper Eqs. A21 and A22 of Ebenhöh et al. (2014), we intend in our future studies to apply these new findings to improve the simulation of the slow SMT phase of fluorescence transient.

Finally, the activation rates of PSII and PSI will be (see also Table 3):

$$k_{\mathrm{LII}} = \mathrm{cPFD} \cdot \mathrm{csII} \cdot \mathrm{PFD} \quad \text{(A23)}$$

$$k_{\mathrm{LI}} = \mathrm{cPFD} \cdot \mathrm{csI} \cdot \mathrm{PFD} = \mathrm{cPFD} \cdot (1 - \mathrm{csII}) \cdot \mathrm{PFD} \quad \text{(A24)}$$

where, PFD is the photon flux density (measured in μmol photons $\mathrm{m}^{-2}\ \mathrm{s}^{-1}$); and cPFD is a constant (here we used cPFD = 1).

With these parameters, the absorption cross section of the antenna, during illumination, reaches a stationary value that depends on the redox state of the PQ pool.

In Ebenhöh et al. (2014) model, Chl *a* fluorescence yield was, for simplicity, assumed to be emitted only by PSII, and it was defined as

$$F2 = \mathrm{csII} \cdot \left(\frac{k_{\mathrm{F}}}{k_{\mathrm{F}} + k_{\mathrm{D}} + k_{\mathrm{Pchem}}} \cdot b_0 + \frac{k_{\mathrm{F}}}{k_{\mathrm{F}} + k_{\mathrm{D}}} \cdot b_{\mathrm{c}}\right). \quad \text{(A25)}$$

Note that, compared with the formula for $F2$ given in the main text (i.e., Eq. 1), here $\mathrm{PSII}_{\mathrm{open}}$ and $\mathrm{PSII}_{\mathrm{closed}}$ were approximated with b_0 and b_{c}, respectively, since b_1 and b_3 acquire very small values (i.e., $\sim 10^{-7}$) during the fluorescence transient.

In this case, the initial PSII fluorescence ($F02$) of a sample in state 1 without qE, when csII = 0.8, $b_0 = 2.5$, $b_{\mathrm{c}} = 0$, and $k_{\mathrm{D}} = k_{\mathrm{Dconst}}$, will be $2k_{\mathrm{F}}/(k_{\mathrm{F}} + k_{\mathrm{Dconst}} + k_{\mathrm{Pchem}})$.

In our paper, however, we have also taken into consideration the Chl *a* fluorescence emitted by PSI (i.e., $F1$). We have assumed that initially, when $F2 = F02$, csI = 0.2, and $k_{\mathrm{D}} = k_{\mathrm{Dconst}}$, PSI fluorescence ($F01$) is 10 % of F_0 (Papageorgiou 1975; Franck et al. 2002), where $F_0 = F02 + F01$; in this case, $F01 = (1/10)(F02 + F01)$, and thus $F01 = (1/9)F02$. Assuming that PSI does not show variable fluorescence (see Lazár 2013 for a different opinion), and depends only on PSI relative absorption cross section (i.e., csI = 1 − csII), and replacing $F02$ with $2k_{\mathrm{F}}/(k_{\mathrm{F}} + k_{\mathrm{Dconst}} + k_{\mathrm{Pchem}})$, $F1$ will be:

$$F1 = \frac{2}{9}\left(\frac{1 - \mathrm{csII}}{0.2}\right) \cdot \frac{k_{\mathrm{F}}}{k_{\mathrm{F}} + k_{\mathrm{Dconst}} + k_{\mathrm{Pchem}}}. \quad \text{(A26)}$$

Finally, we have calculated the total Chl *a* fluorescence as: $F = F2 + F1$.

References

Alami M, Lazár D, Green BR (2012) The harmful alga *Aureococcus anophagefferens* utilizes 19′-butanoyloxyfucoxanthin as well as xanthophyll cycle carotenoids in acclimating to higher light intensities. Biochim Biophys Acta 1817(9):1557–1564

Aliverti A, Jansen T, Zanetti G, Ronchi S, Herrmann RG, Curti B (1990) Expression in *Escherichia coli* of ferredoxin-NADP^+ reductase from spinach. Bacterial synthesis of the holoflavoprotein and of an active enzyme form lacking the first 28 amino acid residues of the sequence. Eur J Biochem 191(3):551–555

Aliverti A, Pandini V, Zanetti G (2004) Domain exchange between isoforms of ferredoxin-NADP^+ reductase produces a functional enzyme. Biochim Biophys Acta 1696(1):93–101

Allakhverdiev SI, Tsuchiya T, Watabe K, Kojima A, Los DA, Tomo T, Klimov VV, Mimuro M (2011) Redox potentials of primary electron acceptor quinone molecule (QA)- and conserved energetics of photosystem II in cyanobacteria with chlorophyll *a* and chlorophyll *d*. Proc Natl Acad Sci USA 108(19):8054–8058. doi:10.1073/pnas.1100173108

Allakhverdiev SI, Tomo T, Stamatakis K, Govindjee (2015) International conference on ''Photosynthesis research for sustainability-2015'' in

honor of George C. Papageorgiou, September 21–26, 2015, Crete, Greece. Photosynth Res. doi:10.1007/s11120-015-0207-9
Allen JF (1992) Protein phosphorylation in regulation of photosynthesis. Biochim Biophys Acta 1098:275–335
Allen JF (2003) Cyclic, pseudocyclic and noncyclic photophosphorylation: new links in the chain. Trends Plant Sci 8:15–19
Allen JF, Bennett J, Steinback KE, Arntzen CJ (1981) Chloroplast protein phosphorylation couples plastoquinone redox state to distribution of excitation-energy between photosystems. Nature 291:25–29. doi:10.1038/291025a0
Allorent G, Tokutsu R, Roach T, Peers G, Cardol P, Girard-Bascou J, Finazzi G (2013) A dual strategy to cope with high light in *Chlamydomonas reinhardtii*. Plant Cell 25:545–557
Alric J (2010) Cyclic electron flow around photosystem I in unicellular green algae. Photosynth Res 106:47–56. doi:10.1007/s11120-010-9566-4
Andersson B, Åkerlund HE, Jergil B, Larsson C (1982) Differential phosphorylation of the light-harvesting chlorophyll–protein complex in appressed and non-appressed regions of the thylakoid membrane. FEBS Lett 149:181–185
Antal TK, Kovalenko IB, Rubin AB, Tyystjärvi E (2013) Photosynthesis-related quantities for education and modeling. Photosynth Res 117:1–30
Bennett J, Steinback KE, Arntzen CJ (1980) Chloroplast phosphoproteins: regulation of excitation energy transfer by phosphorylation of thylakoid membrane polypeptides. Proc Natl Acad Sci USA 77:5253–5257
Böhme H (1978) Quantitative determination of ferredoxin, ferredoxin-$NADP^+$ reductase and plastocyanin in spinach chloroplasts. Eur J Biochem 83(1):137–141. doi:10.1111/j.1432-1033.1978.tb12077.x
Bonaventura C, Myers J (1969) Fluorescence and oxygen evolution from *Chlorella pyrenoidosa*. Biochim Biophys Acta 189:366–383
Bonente G, Ballottari M, Truong TB, Morosinotto T, Ahn TK, Fleming GR, Niyogi KK, Bassi R (2011) Analysis of LhcSR3, a protein essential for feedback deexcitation in the green alga *Chlamydomonas reinhardtii*. PLoS Biol 9(1):e1000577
Bouges-Bocquet B (1973) Electron transfer between two photosystems in spinach chloroplasts. Biochim Biophys Acta 31:250–256
Briantais JM, Merkelo H, Govindjee (1972) Lifetime of the excited state (τ) in vivo. III. Chlorophyll during fluorescence induction in *Chlorella pyrenoidosa*. Photosynthetica 6:133–141
Briantais J-M, Vernotte C, Picaud M, Krause GH (1979) A quantitative study of the slow decline of chlorophyll *a* fluorescence in isolated chloroplasts. Biochim Biophys Acta 548:128–138
Bulté L, Gans P, Rebeillé F, Wollman FA (1990) ATP control on state transitions in vivo in *Chlamydomonas reinhardtii*. Biochim Biophys Acta 1020:72–80
Butler WL, Kitajima M (1975) Energy transfer between photosystem II and photosystem I in chloroplasts. Biochim Biophys Acta 396:72–85
Cammack R, Rao KK, Bargeron CP, Hutson KG, Andrew PW, Rogers LJ (1977) Midpoint redox potentials of plant and algal ferredoxins. Biochem J 168(2):205–209
Carrillo N, Ceccarelli EA (2003) Open questions in ferredoxin-$NADP^+$ reductase catalytic mechanism. Eur J Biochem 270(9):1900–1915
de Wijn R, van Gorkom HJ (2001) Kinetics of electron transfer from q(a) to q(b) in photosystem II. Biochemistry 40(39):11912–11922
Delosme R, Olive J, Wollman FA (1996) Changes in light energy distribution upon state transitions: an in vivo photoacoustic study of the wild type and photosynthesis mutants from *Chlamydomonas reinhardtii*. Biochim Biophys Acta 1273:150–158
Demmig-Adams B, Garab G, Adams WWI, Govindjee (eds) (2014) Non-photochemical quenching and energy dissipation in plants, algae and cyanobacteria. In: Advances in photosynthesis and respiration, vol 40. Springer, Dordrecht
Drop B, Webber-Birungi M, Fusetti F, Kouřil R, Redding KE, Boekema EJ, Croce R (2011) Photosystem I of *Chlamydomonas reinhardtii* contains nine light-harvesting complexes (Lhca) located on one side of the core. J Biol Chem 286:44878–44887. doi:10.1074/jbc.M111.301101
Duysens LNM, Sweers HT (1963) Mechanism of the two photochemical reactions in algae as studied by means of fluorescence. In: Japanese Society of Plant Physiologists (ed), Studies on microalgae and photosynthetic bacteria. University of Tokyo Press, Tokyo, pp 353–372
Ebenhöh O, Houwaart T, Lokstein H, Schlede S, Tirok K (2011) A minimal mathematical model of nonphotochemical quenching of chlorophyll fluorescence. Biosystems 103(2):196–204
Ebenhöh O, Fucile G, Finazzi G, Rochaix J-D, Goldschmidt-Clermont M (2014) Short-term acclimation of the photosynthetic electron transfer chain to changing light: a mathematical model. Philos Trans R Soc B 369:20130223. doi:10.1098/rstb.2013.0223
Evans MC, Heathcote P (1980) Effects of glycerol on the redox properties of the electron acceptor complex in spinach photosystem I particles. Biochim Biophys Acta 590(1):89–96
Farah J, Rappaport F, Choquet Y, Joliot P, Rochaix J-D (1995) Isolation of a psaf-deficient mutant of *Chlamydomonas reinhardtii*: efficient interaction of plastocyanin with the photosystem I reaction center is mediated by the psaf subunit. EMBO J 14(20):4976–4984
Finazzi G, Furia A, Barbagallo RP, Forti G (1999) State transitions, cyclic and linear electron transport and photophosphorylation in *Chlamydomonas reinhardtii*. Biochim Biophys Acta 1413(3):117–129
Franck F, Juneau P, Popovic R (2002) Resolution of the photosystem I and photosystem II contributions to chlorophyll fluorescence of intact leaves at room temperature. Biochim Biophys Acta 1556:239–246
Goral KT, Johnson MP, Duffy CDP, Brain APR, Ruban AV, Mullineaux CW (2012) Light-harvesting antenna composition controls the macrostructure and dynamics of thylakoid membranes in *Arabidopsis*. Plant J 69:289–301
Govindjee (1995) Sixty-three years since Kautsky: chlorophyll *a* fluorescence. Aust J Plant Physiol 22:131–160
Govindjee, Papageorgiou GC (1971) Chlorophyll fluorescence and photosynthesis: fluorescence transients. In: Giese AC (ed) Photophysiology, vol 6. Academic Press, NY, pp 1–46
Govindjee, Amesz J, Fork DC (eds) (1986) Light emission by plants and bacteria. Academic Press, Orlando
Govindjee, Kern JF, Messinger J, Whitmarsh J (2010) Photosystem II. In: Encyclopedia of life sciences (ELS). Wiley, Chichester. doi:10.1002/9780470015902.a0000669.pub2
Grieco M, Suorsa M, Jajoo A, Tikkanen Aro E-M (2015) Light-harvesting II antenna trimers connect energetically the entire photosynthetic machinery—including both photosystems II and I. Biochim Biophys Acta 1847:607–619
Haldimann P, Strasser RJ (1999) Effects of anaerobiosis as probed by the polyphasic chlorophyll *a* fluorescence rise kinetic in pea (*Pisum sativum L.*). Photosynth Res 62:67–83
Heineke D, Riens B, Grosse H, Hoferichter P, Peter U, Flügge UI, Heldt HW (1991) Redox transfer across the inner chloroplast envelope membrane. Plant Physiol 95(4):1131–1137
Iwai M, Yokono M, Nakano A (2014) Visualizing structural dynamics of thylakoid membranes. Sci Rep 4:3768
Jahns P, Holzwarth AR (2012) The role of the xanthophyll cycle and of lutein in photoprotection of photosystem II. Biochim Biophys Acta 1817:182–193

Jans F, Mignolet E, Houyoux P-A, Cardol P, Ghysels B, Cuiné S, Cournac L, Peltier G, Remacle C, Franck F (2008) A type II NAD(P)H dehydrogenase mediates light-independent plastoquinone reduction in the chloroplast of Chlamydomonas. Proc Natl Acad Sci USA 105(5):20546–20551

Joliot P, Johnson GN (2011) Regulation of cyclic and linear electron flow in higher plants. Proc Natl Acad Sci USA 108(32):13317–13322

Kaňa R, Kotabová E, Komárek O, Sedivá B, Papageorgiou GC, Govindjee, Prášil O (2012) The slow S to M fluorescence rise in cyanobacteria is due to a state 2 to state 1 transition. Biochim Biophys Acta 1817:1237–1247

Kargul J, Turkina MV, Nield J, Benson S, Vener AV, Barber J (2005) Light-harvesting complex II protein CP29 binds to photosystem I of *Chlamydomonas reinhardtii* under State 2 conditions. FEBS 272:4797–4806

Kautsky H, Hirsch A (1931) Neue Versuche zur Kohlensäureassimilation. Naturwissenschaften 19:964

Kirchhoff H, Mukherjee U, Galla H-J (2002) Molecular architecture of the thylakoid membrane: lipid diffusion space for plastoquinone. Biochemistry 41(15):4872–4882

Kirilovsky D (2015) Modulating energy arriving at photochemical reaction centers: orange carotenoid protein-related photoprotection and state transitions. Photosynth Res 126:3–17

Kitajima M, Butler WL (1975) Excitation spectra for photosystem I and photosystem II in chloroplasts and the spectral characteristics of the distribution of quanta between the two photosystems. Biochim Biophys Acta 408:297–305

Kodru S, Nellaepalli S, Malavath T, Devadasu E, Subramanyam R, Govindjee (2013) Does the slow S to M rise of chlorophyll a fluorescence induction reflect transition from state 2 to state 1 in the green alga *Chlamydomonas reinhardtii*? In: 16th International Photosynthesis Congress, St. Louis, MO, USA

Kodru S, Malavath T, Devadasu E, Nellaepalli S, Stirbet A, Subramanyam R, Govindjee (2015) The slow S to M rise of chlorophyll *a* fluorescence induction reflects transition from state 2 to state 1 in the green alga *Chlamydomonas reinhardtii*. Photosynth Res 125(1–2):219–231. doi:10.1007/s11120-015-0084-2

Kono M, Noguchi K, Terashima I (2014) Roles of the cyclic electron flow around PSI (CEF-PSI) and O_2-dependent alternative pathways in regulation of the photosynthetic electron flow in short-term fluctuating light in *Arabidopsis thaliana*. Plant Cell Physiol 55(5):990–1004. doi:10.1093/pcp/pcu033

Kouřil R, Zygadlo A, Arteni AA, de Wit CD, Dekker JP, Jensen PE, Scheller HV, Boekema EJ (2005) Structural characterization of a complex of photosystem I and light-harvesting complex II of *Arabidopsis thaliana*. Biochemistry 44:10935–10940

Laisk A, Eichelmann H, Oja V (2006) C3 photosynthesis in silico. Photosynth Res 90:45–66

Laisk A, Nedbal L, Govindjee (eds) (2009) Photosynthesis in silico: understanding complexity from molecules to ecosystems. Advances in photosynthesis and respiration, vol 29. Springer, Dordrecht

Lambrev PH, Miloslavina Y, Jahns P, Holzwarth AR (2012) On the relationship between non-photochemical quenching and photoprotection of Photosystem II. Biochim Biophys Acta 1817:760–769

Lazár D (1999) Chlorophyll *a* fluorescence induction. Biochim Biophys Acta 1412:1–28

Lazár D (2013) Simulations show that a small part of variable chlorophyll *a* fluorescence originates in photosystem I and contributes to overall fluorescence rise. J Theor Biol 335:249–264

Lazár D (2015) Parameters of photosynthetic energy partitioning. J Plant Physiol 175:131–147

Lemeille S, Rochaix J-D (2010) State transitions at the crossroad of thylakoid signalling pathways. Photosynth Res 106(1–2):33–46

Leverenz RL, Sutter M, Wilson A, Gupta S, Thurotte A, Bourcier de Carbon C, Petzold CJ, Ralston C, Perreau F, Kirilovsky D, Kerfeld CA (2015) A 12 Å carotenoid translocation in a photoswitch associated with cyanobacterial photoprotection. Science 348(6242):1463–1466

Li X-P, Björkman O, Shih C, Grossman A, Rosenquist M, Jansson S, Niyogi KK (2000) A pigment-binding protein essential for regulation of photosynthetic light harvesting. Nature 403:391–395

Mar T, Govindjee, Singhal GS, Merkelo H (1972) Lifetime of the Excited State in vivo. I. Chlorophyll *a* in algae, at room and liquid nitrogen temperature; Rate constants of radiationless deactivation and trapping. Biophys J 12:797–808

Mehler AH (1951) Studies on reactions of illuminated chloroplasts. I. Mechanism of the reduction of oxygen and other Hill reagents. Arch Biochem Biophys 33:65–77. doi:10.1016/0003-9861(51)90082-3

Mohanty P, Govindjee (1973) Effect of phenazine methosulfate and uncouplers on light-induced chlorophyll *a* fluorescence yield changes in intact algal cells. Photosynthetica 7:146–160

Mohanty P, Zilinskas-Braun B, Govindjee (1973) Light-induced slow changes in chlorophyll *a* fluorescence in isolated chloroplasts: effects of magnesium and phenazine methosulfate. Biochim Biophys Acta 292:459–476

Murata N (1969a) Control of excitation transfer in photosynthesis. I. Light-induced change of chlorophyll *a* fluorescence in *Porphyridium cruentum*. Biochim Biophys Acta 172:242

Murata N (1969b) Control of excitation transfer in photosynthesis. II. Magnesium ion-dependent distribution of excitation energy between two pigment systems in spinach chloroplasts. Biochim Biophys Acta 189:171–181

Murata N, Allakhverdiev SI, Nishiyama Y (2012) The mechanism of photoinhibition in vivo: re-evaluation of the roles of catalase, α-tocopherol, non-photochemical quenching, and electron transport. Biochim Biophys Acta 1817:1127–1133

Mus F, Cournac L, Cardettini V, Caruana A, Peltier G (2005) Inhibitor studies on nonphotochemical plastoquinone reduction and H_2 photoproduction in *Chlamydomonas reinhardtii*. Biochim Biophys Acta 1708(3):322–332

Nicholls DG, Ferguson SJ (1997) Bioenergetics. Academic Press, San Diego

Niyogi KK, Truong TB (2013) Evolution of flexible non-photochemical quenching mechanisms that regulate light harvesting in oxygenic photosynthesis. Curr Opin Plant Biol 16(3):307–314

Okayama S (1976) Redox potential of plastoquinone A in spinach chloroplasts. Biochim Biophys Acta 440(2):331–336

Pandey JK, Gopal R (2012) Dimethoate-induced slow S to M chlorophyll a fluorescence transient in wheat plants. Photosynthetica 50(4):630–634

Papageorgiou GC (1975) Chlorophyll fluorescence: an intrinsic probe of photosynthesis. In: Govindjee (ed) Bioenergetics of photosynthesis. Academic Press, New York, pp 319–372

Papageorgiou GC, Govindjee (1968a) Light induced changes in the fluorescence yield of chlorophyll *a* in vivo. I. *Anacystis nidulans*. Biophys J 8:1299–1315

Papageorgiou GC, Govindjee (1968b) Light induced changes in the fluorescence yield of chlorophyll *a* in vivo. II. *Chlorella pyrenoidosa*. Biophys J 8:1316–1328

Papageorgiou GC, Govindjee (eds) (2004) Chlorophyll *a* fluorescence: a signature of photosynthesis, advances in photosynthesis and respiration, vol 19. Springer, Dordrecht

Papageorgiou GC, Govindjee (2011) Photosystem II fluorescence: slow changes—scaling from the past. J Photochem Photobiol, B 104:258–270

Papageorgiou GC, Govindjee (2014) The non-photochemical quenching of the electronically excited state of chlorophyll *a* in plants: definitions, timelines, viewpoints, open questions. In: Demmig-Adams B, Garab G, Adams WWI, Govindjee (eds) Non-photochemical quenching and energy dissipation in plants, algae and cyanobacteria. Advances in photosynthesis and respiration, vol 40. Springer, Dordrecht, pp 1–44

Papageorgiou GC, Tsimilli-Michael M, Stamatakis K (2007) The fast and slow kinetics of chlorophyll *a* fluorescence induction in plants, algae and cyanobacteria: a viewpoint. Photosynth Res 94:275–290

Papageorgiou GC, Stamatakis K, Govindjee (2015) The F0 level of chlorophyll a fluorescence induction: does it reflect a standard and reproducible physiological state? In: International Conference of Photosynthesis Research for Sustainability, Crete, Greece, September 2015

Peers G, Truong TB, Ostendorf E, Busch A, Elrad D, Grossman AR, Hippler M, Niyogi KK (2009) An ancient light-harvesting protein is critical for the regulation of algal photosynthesis. Nature 462(7272):518–521

Pfündel EE, Dilley RA (1993) The pH dependence of violaxanthin deepoxidation in isolated pea chloroplasts. Plant Physiol 101(1):65–71

Pribil M, Pesaresi P, Hertle A, Barbato R, Leister D (2010) Role of plastid protein phosphatase TAP38 in LHCII dephosphorylation and thylakoid electron flow. PLoS Biol 8:e1000288

Rintamäki E, Martinsuo P, Pursiheimo S, Aro E-M (2000) Cooperative regulation of light-harvesting complex II phosphorylation via the plastoquinol and ferredoxin-thioredoxin system in chloroplasts. Proc Natl Acad Sci USA 97:11644–11649

Rochaix J-D (2013) Redox regulation of thylakoid protein kinases and photosynthetic gene expression. Antioxid Redox Signal 18:2184–2201

Rochaix J-D (2014) Regulation and dynamics of the light-harvesting system. Annu Rev Plant Biol 65:287–309

Rosing J, Slater EC (1972) The value of G degrees for the hydrolysis of ATP. Biochim Biophys Acta 267:275–290

Schöttler MA, Kirchhoff H, Weis E (2004) The role of plastocyanin in the adjustment of the photosynthetic electron transport to the carbon metabolism in tobacco. Plant Physiol 136(4):4265–4274. doi:10.1104/pp.104.052324

Seelert H, Poetsch A, Dencher NA, Engel A, Stahlberg H, Muller DJ (2000) Structural biology. Proton-powered turbine of a plant motor. Nature 405:418–419

Sétif PQ, Bottin H (1994) Laser flash absorption spectroscopy study of ferredoxin reduction by photosystem I in *Synechocystis* sp. pcc 6803: evidence for submicrosecond and microsecond kinetics. Biochemistry 33(28):8495–8504

Shapiguzov A, Ingelsson B, Samol I, Andres C, Kessler F, Rochaix J-D, Vener AV, Goldschmidt-Clermont M (2010) The PPH1 phosphatase is specifically involved in LHCII dephosphorylation and state transitions in Arabidopsis. Proc Natl Acad Sci 107:4782–4787

Silverstein T, Cheng L, Allen JF (1993) Chloroplast thylakoid protein phosphatase reactions are redox-independent and kinetically heterogeneous. FEBS Lett 334:101–105

Steinbach G, Schubert F, Kaňa R (2015) Cryo-imaging of photosystems and phycobilisomes in Anabaena sp. PCC 7120 cells. J Photochem Photobiol B 142:395–399

Stirbet A, Govindjee (2012) Chlorophyll *a* fluorescence induction: understanding the thermal phase, the J-I-P rise. Photosynth Res 113:15–61

Stirbet A, Riznichenko GYu, Rubin AB, Govindjee (2014) Modeling chlorophyll *a* fluorescence transient: relation to photosynthesis. Biochemistry (Moscow) 79:291–323

Strasser RJ, Govindjee (1991) The Fo and the O-J–I–P fluorescence rise in higher plants and algae. In: Argyroudi-Akoyunoglou JH (ed) Regulation of chloroplast biogenesis. Plenum Press, New York, pp 423–426

Strasser RJ, Srivastava A, Govindjee (1995) Polyphasic chlorophyll *a* fluorescence transient in plants and cyanobacteria. Photochem Photobiol 61:32–42

Suzuki S, Sakurai T, Nakajima T (1987) Characterization of plastocyanin isolated from *Brazilian elodea*. Plant Cell Physiol 28(5):825–831

Tikhonov AN (2015) Induction events and short-term regulation of electron transport in chloroplasts: an overview. Photosynth Res. doi:10.1007/s11120-015-0094-0

Tikhonov AN, Vershubskii AV (2014) Computer modeling of electron and proton transport in chloroplasts. BioSystems 121:1–21

Tokutsu R, Minagawa J (2013) Energy-dissipative supercomplex of photosystem II associated with LHCSR3 in *Chlamydomonas reinhardtii*. Proc Natl Acad Sci USA 110:10016–10021

Tsimilli-Michael M, Stamatakis K, Papageorgiou GC (2009) Dark-to-light transition in *Synechococcus* sp. PCC 7942 cells studied by fluorescence kinetics assesses plastoquinone redox poise in the dark and photosystem II fluorescence component and dynamics during state 2 to state 1 transition. Photosynth Res 99:243–255

Tyystjärvi E (2013) Photoinhibition of photosystem II. Int Rev Cell Mol Biol 300:243–303

Tyystjärvi E, Hakala M, Sarvikas P (2005) Mathematical modelling of the light response curve of photoinhibition of photosystem II. Photosynth Res 84:21–27

Usuda H (1988) Adenine nucleotide levels, the redox state of the NADP system, and assimilatory force in nonaqueously purified mesophyll chloroplasts from maize leaves under different light intensities. Plant Physiol 88:1461–1468

Van der Veen R (1949) Induction phenomena in photosynthesis -I. Physiol Plant 2:217–234

Walker DA (1992) Concerning oscillations. Photosynth Res 34:387–395

Witt H, Bordignon E, Carbonera D, Dekker JP, Karapetyan N, Teutloff C, Webber A, Lubitz W, Schlodder E (2003) Species-specific differences of the spectroscopic properties of P700: analysis of the influence of non-conserved amino acid residues by site-directed mutagenesis of photosystem I from *Chlamydomonas reinhardtii*. J Biol Chem 278(47):46760–46771. doi:10.1074/jbc.M304776200

Wlodarczyk LM, Snellenburg JJ, Ihalainen JA, van Grondelle R, van Stokkum IHM, Dekker JP (2015) Functional rearrangement of the light-harvesting antenna upon state transitions in a green alga. Biophys J 108(2):261–271

Zaks J, Amarnath K, Kramer DM, Niyogi KK, Fleming GR (2012) A kinetic model of rapidly reversible nonphotochemical quenching. Proc Natl Acad Sci USA 109(39):15757–15762. doi:10.1073/pnas.1211017109

Zhao W, Xie J, Xu X, Zhao J (2015) State transitions and fluorescence quenching in the cyanobacterium Synechocystis PCC 6803 in response to changes in light quality and intensity. J Photochem Photobiol B 142:169–177

Zhou Y, Schideman CL, Rupassara SI, Govindjee, Seufferheld MJ (2010) Improving the photosynthetic productivity and light utilization in algal biofuel systems: metabolic and physiological characterization of a potentially advantageous mutant of *Chlamydomonas reinhardtii*. In: 15th International Photosynthesis Congress, Beijing, China

Zhou Y, Schideman LC, Park DS, Stirbet A, Govindjee Rupassara SI, Krehbiel JD, Seufferheld MJ (2015) Characterization of a *Chlamydomonas reinhardtii* mutant strain with improved

biomass production under low light and mixotrophic conditions. Algal Res 11:134–147

Zhu XG, Wang Y, Ort DR, Long SP (2013) e-photosynthesis: a comprehensive dynamic mechanistic model of C3 photosynthesis: from light capture to sucrose synthesis. Plant, Cell Environ 36:1711–1727

Zito F, Finazzi G, Delosme R, Nitschke W, Picot D, Wollman FA (1999) The Qo site of cytochrome *b6f* complexes controls the activation of the LHCII kinase. EMBO J 18:2961–2969. doi:10.1093/emboj/18.11.2961